Study of the Reactivity of CH3COOH+. and COOH+ Ions with CH3NH2: Evidence of the Formation of New Peptide-like C(O)-N Bonds

Imene Derbali, R. Thissen, Christian Alcaraz, Claire Romanzin, Emilie-Laure Zins

▶ **To cite this version:**

Imene Derbali, R. Thissen, Christian Alcaraz, Claire Romanzin, Emilie-Laure Zins. Study of the Reactivity of CH3COOH+. and COOH+ Ions with CH3NH2: Evidence of the Formation of New Peptide-like C(O)-N Bonds. Journal of Physical Chemistry A, 2021, 125 (46), pp.10006-10020. 10.1021/acs.jpca.1c06630 . hal-03451178

HAL Id: hal-03451178
https://hal.science/hal-03451178v1

Submitted on 9 Nov 2022

HAL is a multi-disciplinary open access archive for the deposit and dissemination of scientific research documents, whether they are published or not. The documents may come from teaching and research institutions in France or abroad, or from public or private research centers.

L'archive ouverte pluridisciplinaire **HAL**, est destinée au dépôt et à la diffusion de documents scientifiques de niveau recherche, publiés ou non, émanant des établissements d'enseignement et de recherche français ou étrangers, des laboratoires publics ou privés.

Study of the Reactivity of $CH_3COOH^{+\bullet}$ and $COOH^+$ Ions With CH_3NH_2 : Evidence of the Formation of New Peptide-like C(O)-N Bonds

Imene Derbali,[a] Roland Thissen, [b,c*] Christian Alcaraz, [b,c] Claire Romanzin, [b,c] Emilie-Laure Zins [a *]

a: Sorbonne Université, CNRS, De la Molécule aux Nano-Objets: Réactivité, Interactions Spectroscopies, MONARIS, 75005, Paris, France

b: Institut de Chimie Physique, Bât. 350, UMR 8000, CNRS-Univ. Paris Saclay, Orsay, France

c: Synchrotron SOLEIL, L'Orme des Merisiers, Saint-Aubin—BP 48, Gif-sur-Yvette, France

*: Corresponding authors, roland.thissen@universite-paris-saclay.fr, emilie-laure.zins@sorbonne-universite.fr

Abstract

Acetamide, a small organic compound containing a peptide bond, was observed in the interstellar medium, but reaction pathways leading to the formation of this prebiotic molecule remain uncertain. We investigated the possible formation of a peptide-like bond from the reaction between acetic acid (CH_3-COOH) and methylamine (CH_3-NH_2), that were identified in the interstellar medium. From an experimental point of view, a Quadrupole / Octopole / Quadrupole mass spectrometer was used in combination with Synchrotron radiation as tunable source of VUV photons for monitoring the reactivity of selected ions. Acetic acid was photoionized, and the reactivity of $CH_3COOH^{+\bullet}$ as well as $COOH^+$ (produced either from acetic or formic acid) ions with neutral CH_3NH_2 was further studied. With no surprise, charge transfer, proton transfer, and concomitant dissociation processes were found to largely dominate the reactivity. However, a C(O)-N bond formation process between the two reactants was also evidenced, with a weak cross section reaction. From a theoretical point of view, results concerning reactivity and barrier heights were obtained using density functional theory, with the LC-ωPBE range-separated functional in combination with the 6-311++G(d,p) Pople basis set and are in perfect agreement with the experimental data.

I. Introduction

As telescopes become more sophisticated and space missions for in situ collection or analysis of molecules increase, we are discovering more and more molecules involving complex chemical reactions. So-called complex organic molecules (COM) detected in the insterstellar medium, in icy dust grains and in the comaes of comets are carbon-bearing molecules with at least six atoms.[1] COM include a wide range of prebiotic molecules such as sugars (glycolaldehyde),[2,3] carboxylic acids and amines.

Among primary amines, formamide NH_2CHO was identified as early as 1971 in the SGR B2 cloud,[4] followed three years later by methylamine CH_3NH_2 identified in the SGR B2 and Orion A clouds, while hydroxylamine NH_2OH was recently identified (2020) in the quiescent molecular cloud G+0.693-0.027.[5] Methylamine has also been detected in the comet 67P/Churyumov-Gerasimenko by the Rosetta

mission.[6,7,8] This mission also detected glycine and alanine in the same comet 67P/Churyumov-Gerasimenko.[6,7,8] Among carboxylic acids, formic acid HCOOH was the first to be detected in the interstellar medium (1971, SGR B2 cloud[9]), and it was only in 1997 that acetic acid CH_3COOH was detected in the SGR B2, Orion KL and W51 clouds.[10]

Paradoxically, in spite of increasingly in-depth studies, issues concerning the reaction mechanisms involved in the chemistry of these media are ever-increasing: how are such complex molecules formed ? Is the chemistry of the interstellar medium dominated by mechanisms catalyzed in solid phase by dust grains (purely mineral or mixed with water ice) frozen at very low temperature (T<20K) ? Are higher temperature gas phase processes also involved ? It seems obvious that interstellar dust grain processes play an important role, including in the mechanisms of formation of comet constituents. However, a thorough study of the volatiles and refractory materials that were captured during the Stardust mission also revealed the role of gas-phase reactions at higher temperatures.[6,7,8] Theoretical and laboratory experimental studies under varied and complementary conditions are clearly still required for the elucidation of these processes. Such laboratory studies are fundamental to improve our understanding of chemical reactions in extreme environments. Numerous studies have made it possible to propose mechanisms for some of the chemical species that have been identified in space, but we are still far from having a complete and satisfactory model to explain all the reactions, and systematic laboratory studies seem to be indispensable, both from a theoretical and experimental point of view.[11,12]

From a prebiotic point of view, the detection of carboxylic acids and amines in interstellar medium (ISM) is very interesting because it opens the way to reactions that can lead to the formation of new peptide-like C(O)-N bonds (*Scheme 1*).

In addition, the study of such reaction mechanisms would also allow to better describe the formation of atmospheric aerosols, [13-17] the formation of prebiotic molecules in hot-cores, hot-corinos[18] and in complex environments, [19-24] as well as to contribute to more fundamental studies on reactivity[25].

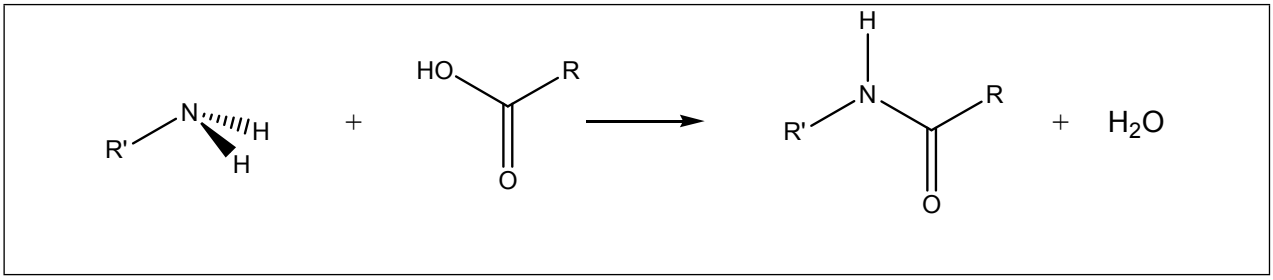

***Scheme 1*: Reactions of the peptide bond formation between a carboxylic acid and an amine.**

An energy barrier of about 150 kJ/mol (1.55 eV) is often associated with the formation of this bond in the gas phase. In line with this energy barrier, the formation of a C(O)-N bond at the molecular level, from a carboxylic acid and an amine taken in their fundamental state has not yet been demonstrated experimentally, to our knowledge.[26,27,28] This is why it has been proposed, in the context of prebiotic chemistry, that this reaction could be catalyzed by surfaces such as siliceous clays or meteorite rocks. Moreover, G. Bouchoux et al.[29] showed that in the presence of one to four water molecules the energy barrier associated with the reaction of NH_3 or NH_4^+ on formic acid was strongly lowered. An explicit role of water in the reaction process was further demonstrated by the authors.

The aim of this work is to initiate an in-depth research on the binding formation conditions of a peptide-like type bond from reagents of prebiotic interest taken in their fundamental state, or in weakly excited states. We present here a first part of this work as two independent papers. This first article is dedicated to the highlighting of the formation of a C(O)-N bond from $CH_3COOH^{+\bullet}$ or $COOH^+$ with CH_3NH_2 using a

coupled theoretical/experimental approach. The second article[30] is dedicated to the introduction of a new methodology for the algorithmic investigation of reaction paths for the formation of CH_3-NH-CO-CH_3 from neutral CH_3NH_2 and CH_3COOH isolated in the gas phase with or without the presence of a few explicit water molecules.

For this first study, synchrotron radiation was used as a tunable source of VUV photons. This makes it possible to monitor the potential effect of internal energy of prepared cations and radical cations. The $CH_3COOH^{+\bullet}$ and $COOH^+$ cations formed from CH_3COOH and/or HCOOH precursors were then selected in mass using a mass spectrometer. The addition of the neutral CH_3NH_2 partner in a reaction chamber before detection of the formed species allows the identification of the reaction products as a function of the energy of the photons used for the photoionization or the dissociative photoionization step. The absolute cross sections of the reaction were derived from a multi-step methodological approach, involving the following steps:

1. the recording of spectra of ionized species in the absence of reactive gas,
2. the study of metastable fragmentation, and collision-induced ion fragmentation in the presence of a chemically (relatively) inert target: argon,
3. the study of the products obtained in the presence of the reagent as a function of photon energy and collision energy,
4. the comparison of spectra obtained in steps 2 and 3 to characterize the reactivity.

To help identifying the products formed under experimental conditions, it is essential to carry out a theoretical study of the reaction pathways. For this study, we have chosen Density Functional Theory (DFT) calculations. In addition to proton transfer, charge transfer and hydride transfer processes, this double theoretical and experimental approach has allowed us to highlight for the first time C(O)-N bond formation reactions between ions formed from carboxylic acids and methylamine.

II. Methods

a. Experimental approach

The experiments have been performed using the CERISES apparatus, an associated experiment to the SOLEIL synchrotron radiation facility. Since the set-up was described in details previously, only the most relevant details will be given here.[31,32] CERISES is a guided ion beam tandem mass spectrometer composed of two octopoles located between two quadrupole mass spectrometers in a Q1-O1-O2-Q2 configuration that permits investigation of bi-molecular reactions of mass-selected ions occuring in a 4cm long reaction cell located at the end of the first octopole. By measuring the yields of parent- and product-ions, absolute reaction cross sections and branching ratios as a function of both photon- and collision energy are derived.

$CH_3COOH^{+\bullet}$ and $HCCO^+$ reactant ions were produced by dissociative photoionization of their gaseous precursor introduced at roughly 10^{-6} mbar in the ion source of CERISES connected to the DESIRS beamline of SOLEIL synchrotron. The undulator-based DESIRS beamline provides tunable radiation in the vacuum ultraviolet (VUV) range from 5 to 40 eV.[33] Photons at the desired energies are selected and scanned simultaneously with the undulator peak energy by a normal incidence monochromator equipped with a low dispersion uncoated SiC grating (200 grooves/mm) optimized to provide photon flux up to 10^{13} photon/s. In the present experiments, the photon energies required to produce and react the ions are in the range 10–15.5 eV. The monochromator slits were set in the range 300 to 600 µm, corresponding to a resolution of 20 to 40 meV, compromizing for a maximum of signal and avoiding detector saturation. The monochromator was operated at its first order of diffraction. Higher orders were removed from the

incident beam by use of a gas filter installed on the beam line filled with argon at a pressure of 0.2 mbar as absorber.[34] This removes efficiently any photons above 15.7 eV. The absolute scale of the photon energies was checked by using sharp absorption lines of atomic Argon around 11.828 and 14.304 eV that were observed with systematic shifts of about 10-20 meV above their tabulated values.[35,36]

The kinetic energy of the parent ion, and hence the collision energy, was set by the difference between the ion source and the reaction cell potentials. This was determined by the stopping potential method on the parent ion beam, giving a kinetic energy width of 400 meV FWHM, on average. By changing the potentials of the reaction cell and all subsequent elements, the kinetic energy of the parent ion was increased up to 20 eV in the lab, corresponding to a collision energy of 6.5 and 8 eV in the center of mass frame and a width of 130-160 meV for the reactions 1 and 2, respectively:

$CH_3COOH^{+\bullet} + CH_3NH_2$ (Reaction 1)

$COOH^{+} + CH_3NH_2$ (Reaction 2)

The resolution of quadrupole mass filters was compromized in order to have good signals as well as sufficient removal of ions at + or – 1 mass unit from the considered species. Our estimate is a removal of 99.99% of neighbour ions for Q1 and 99.90% of neighbour ions for Q2 at the lowest collision energy with a loss of performance reaching 98.80% of neighbour ions when operated at the highest collision energy.

Methylamine (and argon for the CID study) was introduced in the cell at a pressure of up to 200 nbar, which allows to consider essentially single collision processes over the 4 cm long reaction cell by keeping secondary reactions at reduced level, but still provides with accurate pressure measurements and large detection dynamics on reaction cross section between 200 and 0.01 Å². The absolute pressure in the cell was measured using the MKS 398H differential manometer instrument. All data were collected with either reaction gas in the cell or in the surrounding chamber, therefore allowing for the removal of any signal resulting from collisions occurring outside the reaction cell, corresponding at maximum to 5 % of the total reactivity signal.

The absolute cross sections acquisition method, either for photon or collision energy scans, was performed in so-called multiscan mode, which implies recording signals for all ionic species at a single point before to move to the next point. This method reduces drastically effects of drifts in source pressure, reaction cell pressure or photon flux.

The CERISES apparatus being a tandem instrument, it is possible to derive information on metastable processes related to the ion produced in the source, mass-selected with Q1, and let to fly freely through O1 and O2. Potential metastable products can then be detected with Q2. Such measurements were performed in the case of acetic acid cation selected at m/z=60, and producing metastable products at m/z=42. In our experimental conditions, the flight time for those ions to reach the end of Q1 is 161µs. Three measurements performed at acceleration potentials of 0.25, 2 and 12V correspond to flight times at the end of O2 of m/z=60 ion of 460, 381 and 261µs, respectively.

The chemicals (acetic acid, formic acid, and methylamine) were purchased from Sigma Aldrich at chromatographic grade (99.8%) and used without further purification.

b. Theoretical approach

All the calculations were performed with the Gaussian09 software (revision D.01).[37] The DFT approach, [38, 39, 40,] which allows a good compromise between reliability of results and calculation time, has been chosen

here. Since the reaction paths may involve the formation of non-covalent complexes between reagents, the LC-ωPBE[41,42,43] range separation functional was used with the empirical correction GD3BJ proposed by Becke and Johnson, and formalized by Grimme.[44] These calculations were performed using the triple ζ Pople basis 6-311++G(d,p).[45] In addition, the following calculation options were used: scf=(Tight,MaxCycle=500) Int=UltraFine opt=(MaxCycle=500). The reliability of such level of theory was previously benchmarked by Grimme et al. and Dilabio et al.[46,47]

The nature (local minimum or transition state) of the stationary points was determined by performing a frequency calculation at the same calculation level as the optimization. For the C(O)-N bond formation reactions, the potential energy surface was investigated by performing an Intrinsic Reaction Coordinate (IRC) calculation from the transition state. For the reaction paths involving simple breaks, relaxed scans were performed. The ZPE correction was only taken into account for stationary points.

III. Experimental evidence for bond-forming reactions

a. Background

Evidence of the formation of new chemical bonds from isolated species in the gas phase taken in their fundamental state remains relatively rare. The use of mass spectrometry coupled with synchrotron radiation allows the preparation of cation radicals with tunable internal energy. These species can then be selected in mass, and their reactivity can be probed as a function of the energy of the ionizing photons. The dications have thus been shown to be highly reactive, even in their fundamental state.[48,49] Bond formations were found with different neutral unsaturated reagents such as benzene,[49,50] as well as small molecules such as methane,[48] CO_2, H_2O, HCl, N_2, O_2,[51 52] or rare gases[53] for example. This wide range of reactivity of the dications has led to the introduction of the "super-electrophiles" concept. The formation of new chemical bonds by reaction between a monocation and a neutral species has been the subject of numerous studies. It should be noted, however, that these systems mainly lead to proton, hydride or atomic hydrogen transfers or charge transfers rather than to the formation of new chemical bonds between the two partners. As in the case of dications, it is often unsaturated species that lead to the formation of new chemical bonds. Thus, regarding the reactivity of neutral methylamine with a monocation, some of the reactions that have been studied are presented in *Table 1*.

Reagent	Observed mechanism	Reference
HCN^+	PT	
$HCNH^+$	PT, CT, H^-T, adduct	54, 55
$HCNH_2^+$	PT, CT, H^-T	55
$CH_2NH_2^+$	PT, CT, H^-T, adduct	54
$CH_3NH_2^+$	PT, CT, H^-T, adduct	54
$CH_3NH_2D^+$	PT	
$(CH_3)_2NH_2^+$	PT	
$(CH_3CN)_2H^+$	PT, exchange in an adduct, adduct	
$CH_3OCH_2^+$	$CH_3NHCH_2^+ + CH_3OH$ $(CH_3)_2NH_2^+ + H_2CO$	56
$C_2H_5OH_2^+$	PT	
$(C_2H_5OH)_2H^+$	exchange in an adduct	
$(C_2H_5OH)_3H^+$	exchange in an adduct	
H_2CCHCO^+	PT, adduct	
$HCCCHOH^+$	PT, adduct	
c-$C_6H_5OH^+$	PT	
$CH(OH)_2^+$	PT	
$CH_3C(OH)_2^+$	PT	

$((CH_3)_2O)_2H^+$	PT, exchange in an adduct	
$((CH_3)_2CO)_2H^+$	exchange in an adduct, adduct	
$H(CH_3COH)_3^+$	exchange in an adduct	
$(CHOOH)_2H^+$	exchange in an adduct	
$(CH_3COOH)_2H^+$	adduct	
$(CH_3COOCH_3)_2H^+$	exchange in an adduct, adduct	
$(C_8H_{17}O_4(CH_3OH)^+$	Insertion in a crown ether	57
$(CHOOH)_3H^+$	PT, exchange in an adduct	
$(CH_3COOH)_3H^+$	PT, exchange in an adduct, adduct	

***Table 1*: Compilation of ion-molecule reactions involving methylamine reported in the Anicich database.[58] PT, CT and H$^-$T stand for proton transfer, charge transfer and hydride transfer, respectively.**

To our knowledge, no reaction has been carried out on a cation (not an adduct) containing a carboxylic acid function and an amine. The first step of our work was to determine whether, in addition to proton, hydride or charge transfer processes, reactions leading to the formation of new chemical bonds between the cation and the amine occurred.

As stated in the introduction, the derivation of the absolute cross-sections of the reaction requires a multi-step process. It seemed essential to present the main results of the different steps under our experimental conditions, although some aspects have been previously studied by other groups (such as the metastability of the parent ion $CH_3COOH^{+\bullet}$, and its collision induced dissociation in the presence of argon [59]). We were thus first interested in the ionization threshold of acetic acid, then in the metastability of the parent ion $CH_3COOH^{+\bullet}$, and its dissociation induced by collision with an inert partner, argon.

As a comparison, we were also interested in the formation and reaction of the $COOH^+$ ion from formic acid. Therefore the ionization threshold of formic acid, the metastability of the $COOH^+$ ion, and its dissociation induced by collision with argon were also studied.

Photoionization of acetic acid

In perfect agreement with the previous studies, the main ionic channels observed are the following (*Figure 1*):

$$CH_3COOH + h\nu \rightarrow CH_3COOH^{+\bullet} \quad m/z = 60$$
$$\rightarrow CH_3^{\bullet} + COOH^+ \quad m/z = 45$$
$$\rightarrow OH^{\bullet} + CH_3CO^+ \quad m/z = 43$$

To better understand these fragmentations, the ion yields as a function of the photon energy have been measured (*Figure 1*). Our combined experimental and theoretical approach allows us to determine the ionization threshold of acetic acid at 10.6 eV (IE_{theo} = 10.64 eV, IE_{exp} = 10.6± 0.05 eV). These results are fully consistent with those of Leach et al. [59] who had experimentally determined an ionization threshold of 10.58 ± 0.02 eV. The first fragmentation process at m/z 43 associated to products CH_3CO^+ and OH appears at 11.5 ± 0.1 eV. For the appearance threshold of the $COOH^+$ fragment at m/z 45, an experimental value of 12.1 ± 0.02 eV is obtained. From a theoretical point of view, the formation of this cation with the concomitant loss of the $CH_3^{\bullet}$ radical, is calculated with a threshold of appearance of 12.27 eV (the optimized structures are presented in SI), which is a good theoretical/experimental agreement, as well as a good consistency with the already-published data.[60]

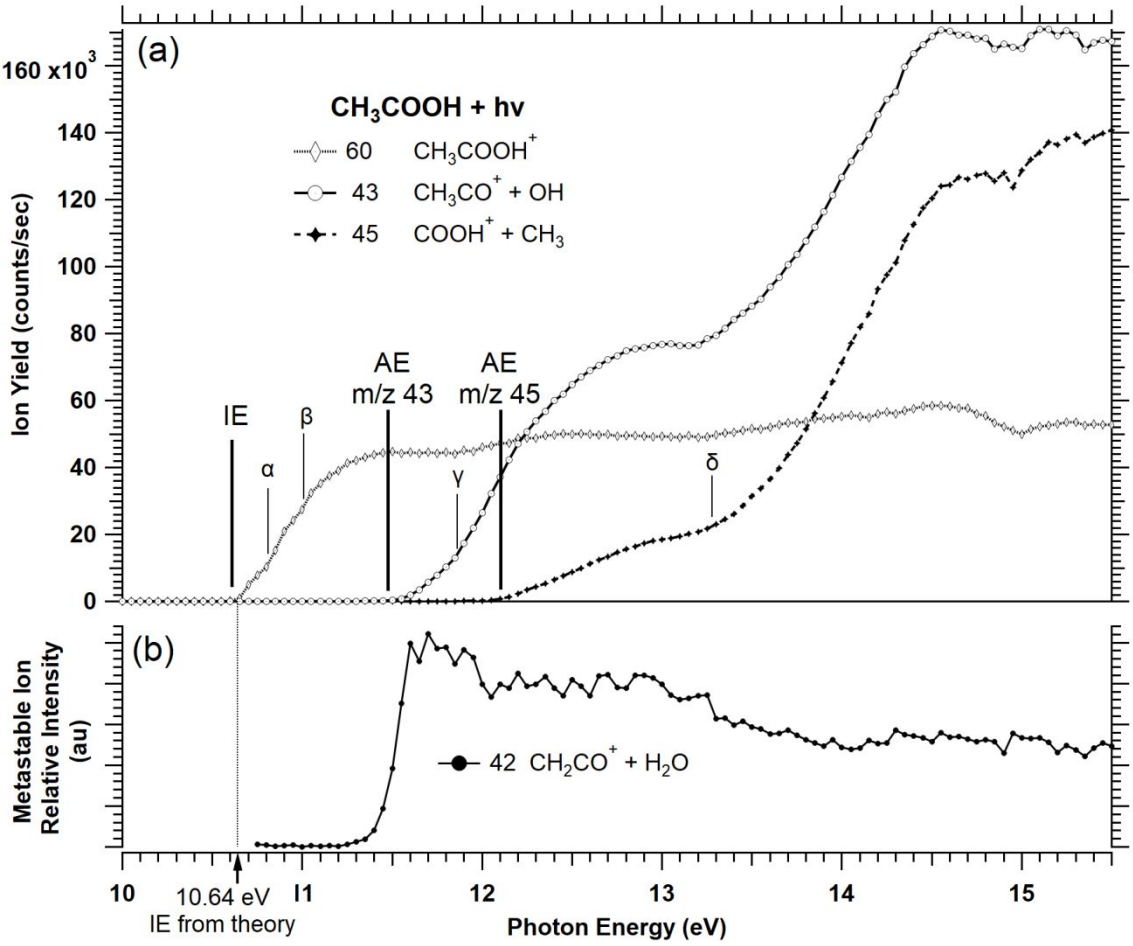

Figure 1: Evolution as a function of the ionizing photon energy for acetic acid of (a) the yields of the three major ionic products, and (b) the metastable process leading to the m/z=42 ion. IE and AE stand for ionization energy and appearance energy, respectively.

Each of the three ion yield curves can be split into several features revealing the spectroscopy:

- two (small) slope breaks (α and β in Figure 1) are observed around 10.8 and 11 eV in the ion yield of the parent ion, which may suggest the populating of vibrationally excited states of the radical cation formed. This is fully consistent with the substructures observed in the 13a' state peak described by Borodin,[61]
- a third (small) slope break (γ in Figure 1) is observed in the ion yield curve of the parent ion, as well as for the ion yield at m/z 43 around 11.85 eV. According to Borodin's work, this corresponds to the population of the electronically excited state 3a'', a state that has an antibonding character on the C=O bond, and probably associated with OH loss,
- a fourth slope break (δ in Figure 1) much more pronounced than the three previous ones, is observed around 13.2 eV for the fragments at m/z 43 and 45. To a lesser extent, this slope break is also observed in the ion yield curve of the parent ion. This is well correlated with the second excited electronic state (2a'') of the ion which also has an antibonding C=O character. Alternatively, this threshold could correspond to the appearance of isomerization, which would open the way to other channels for its dissociative photoionization. But in such a case, we should have observed the formation of new fragmentation pathways for these photon values, which was not the case. Let us notice, because it will be important here after for our discussion of results, that the increase of intensity for the $COOH^+$ fragment beyond this slope break is roughly a factor six to one.

Dissociative photoionization thresholds of formic acid

The photoionization and dissociative photoionization thresholds shown in *figure 2* are consistent with the published data (formic acid ionization threshold around 11.3 eV [62,63,64]). The $HCCOH^+$ ion appears at 11.3 ± 0.05 eV and the $COOH^+$ fragment ion appears at 12.3 ± 0.05 eV.

Here as well, several features are visible in the ion yield curves:

- four (small) steps (α' to δ' in Figure 2) observed between 11.3 and 12.2 eV in the ion yield of the parent ion, which are correlated with population of vibrationally excited (v=1 to 4) states of the radical cation formed in its ground state, 10a'. This is fully consistent with the substructures observed at high resolution by Siggel king et al.[64]
- the second state, 2a", does not exhibit particular structures, but corresponds to the appearance of the $COOH^+$ fragment, of interest in this study.
- The third state, 9a' appears as a broad structure, is visible in the yield of all product ions, and leads to an increase of intensity by roughly a factor two to one for the $COOH^+$ fragment.

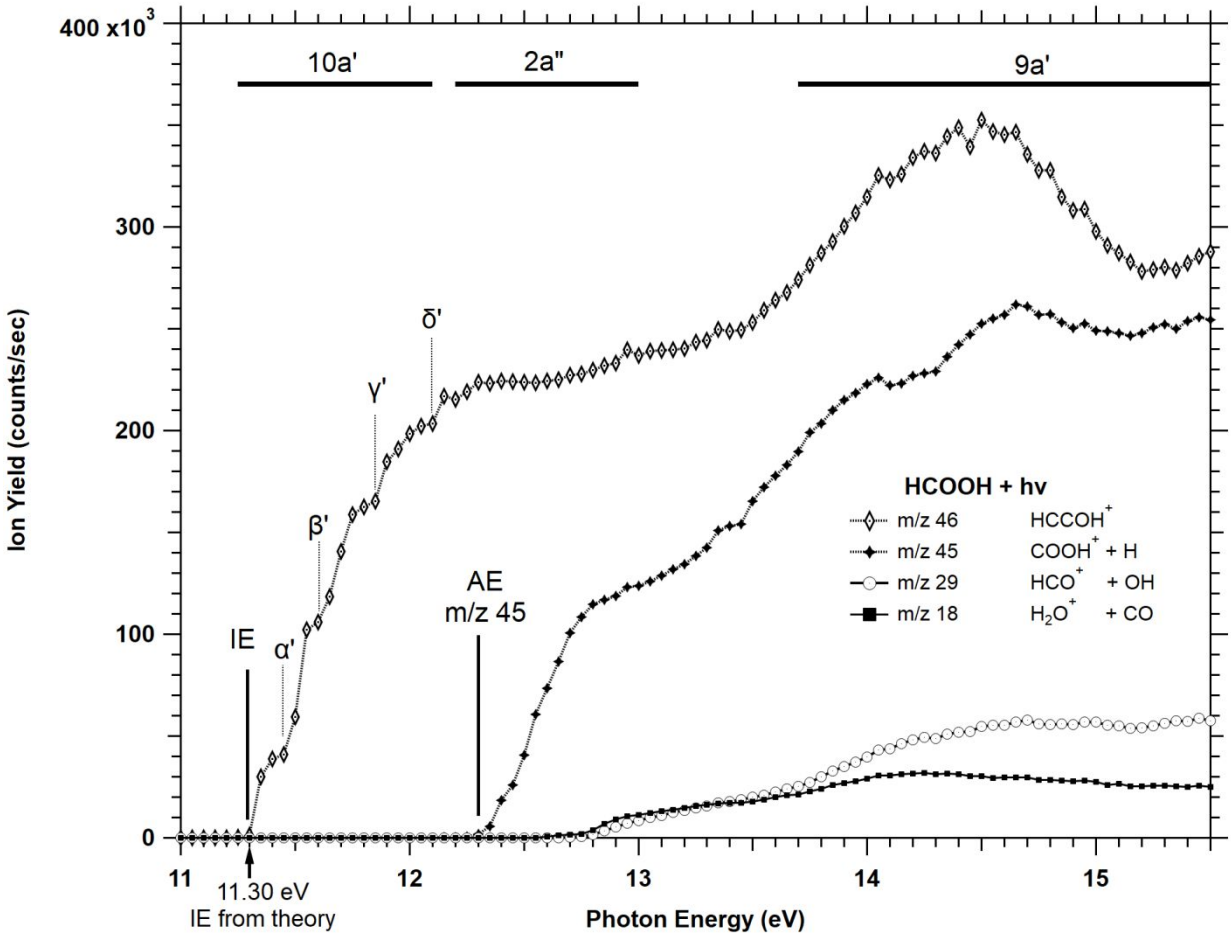

***Figure 2*: Evolution of the ionic yield as a function of the energy of the ionizing photons, for formic acid, and comparison of the theoretical and experimental values obtained for the ionization threshold and for the threshold of appearance of the ion at m/z 45. IE and AE stand for ionization energy and appearance energy, respectively.**

The theoretical and experimental ionization energies of acetic acid and formic acid are compared in the *Table 2*. The theoretical values obtained at the LC-ωPBE+ GD3BJ/6-311++G(d,p) computational level are quite consistent with the experimental values, which further supports our choice of this computational level for this study.

	CH_3COOH	HCOOH
Neutral E_{tot} (Hartree)	-228.961593	-189.675281
Cationic E_{tot} (Hartree)	-228.570768	-189.259876
Theoretical IE (eV)	10.64	11.30
Experimental IE (eV)	10.60 ± 0.05	11.30 ± 0.05

***Table 2*: Comparison of the experimental and theoretical ionization energies of CH_3COOH and HCOOH**

No metastable or CID processes with Ar in the dissociation of the ion m/z 45 were detected within the limit of our collision energy (20 eV lab). This is why in the subsequent section only the metastability of acetic acid will be discussed.

Metastability of $CH_3COOH^{+\bullet}$ ion from acetic acid

Metastability measurements performed by selecting the m/z 60 ion with first quadrupole and recording the ion present in the beam with the second quadrupole, with no reactive gas in the reaction cell, shows that the m/z 42 fragment is produced. This most likely corresponds to the formation of the CH_2CO^+ ion, with the concomitant loss of a water molecule from CH_3COOH^+, as described in the literature.

In our experimental conditions, fragments at m/z 45 and 43 do not appear as metastable products.

As shown in *figure 1b*, the metastable process has an appearance around 11.45 eV. Its relative intensity to the m/z 60 ion reaches a plateau between 11.6 to 12 eV, followed by two steps down observed around 12 and 13.5 eV. These steps correlate with the population of 3a'' and 2a'' states, and hint at a reduced probability to produce the metastable entity when starting from those states. We have recorded such dependency at three different acceleration voltages (0.25, 2 and 12 V) in the octopoles region. When the applied voltage decreases, the residence time of the ions in the octopoles increases, which increases the metastable signals. The three curves are perfectly proportional in the photon energy range studied (11.5 to 15.5 eV) which indicates that there is no evolution of the metastable lifetime when changing the photon energy. Considering simulated flight times for m/z 60 ions in the octopole region at the 3 acceleration voltages, the evolution of metastable signals let us estimate a metastable lifetime of 300 ± 50 µs.

CID of acetic acid with argon

In order to decipher reactions and collision induced process in our system, non-reactive argon was introduced in the reaction cell to characterize collision-induced dissociations. The mass spectra obtained with photons having an energy of 14.5 eV are shown in *figure 3* and reveal product ions at m/z, 42 ($C_2H_2O^+$ + H_2O), 43 ($C_2H_3O^+$ + OH) and 45 (CO_2H^+ + CH_3), the latter two being a clear effect of the collision, while the first one is essentially the metastable signature described before.

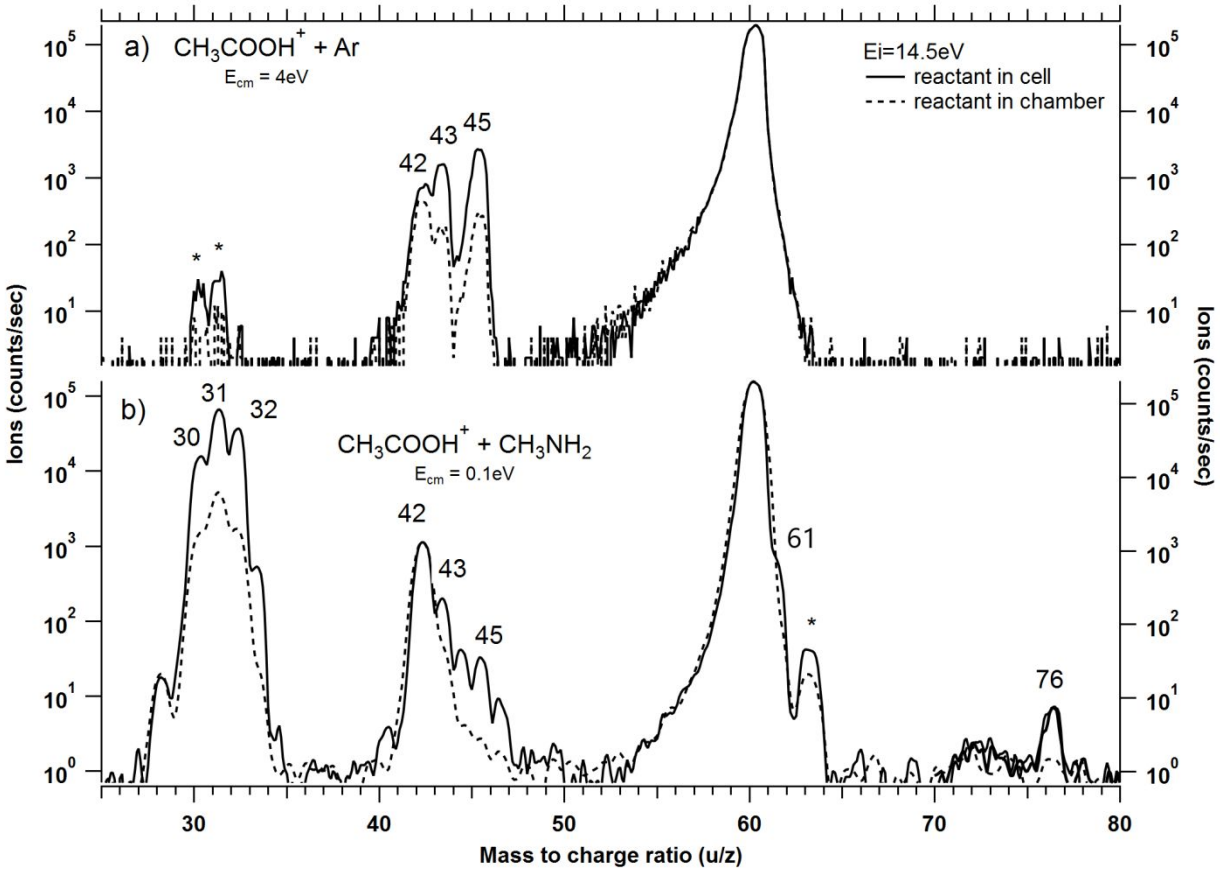

***Figure 3*: Mass spectra recorded at 14.5 eV photon energy, obtained when selecting parent ion at m/z 60 ($CH_3COOH^{+\bullet}$) and colliding in the reaction cell with either argon (a), or methylamine (b). In each case, two spectra are shown with either the reactant gas introduced in the cell (continuous line, left scale) or in the chamber surrounding the cell (dashed line, right scale). The mass region between m/z 70 and 80 in b) has been collected with an increased accumulation time (x10) and is represented with a bold line. Mass peaks indicated with a (*) correspond to ions that cannot be described as result of the considered ion molecule reactions, and most probably result from reactions with remnants of neutral samples previously introduced in the reaction cell.**

Absolute reaction cross sections were determined for the three product ions as a function of collision energy in the center of mass (*Figure 4*). They all three exhibit a threshold behaviour, associated to an increase of yield when increasing the collision energy. It is noticeable that the measurements performed with the ionic target produced close to its ionization energy, i.e. with small internal energy, request for higher collision energy to exhibit the two channels leading to CH_2CO^+ and CH_3CO^+. The $COOH^+$ channel (m/z 45) is not affected at all by the photon energy, indicating that the energy requested to induce this dissociation is hardly provided into the selected m/z 60 ion produced by the photoionization process. The three channels show similar asymptotic behaviour.

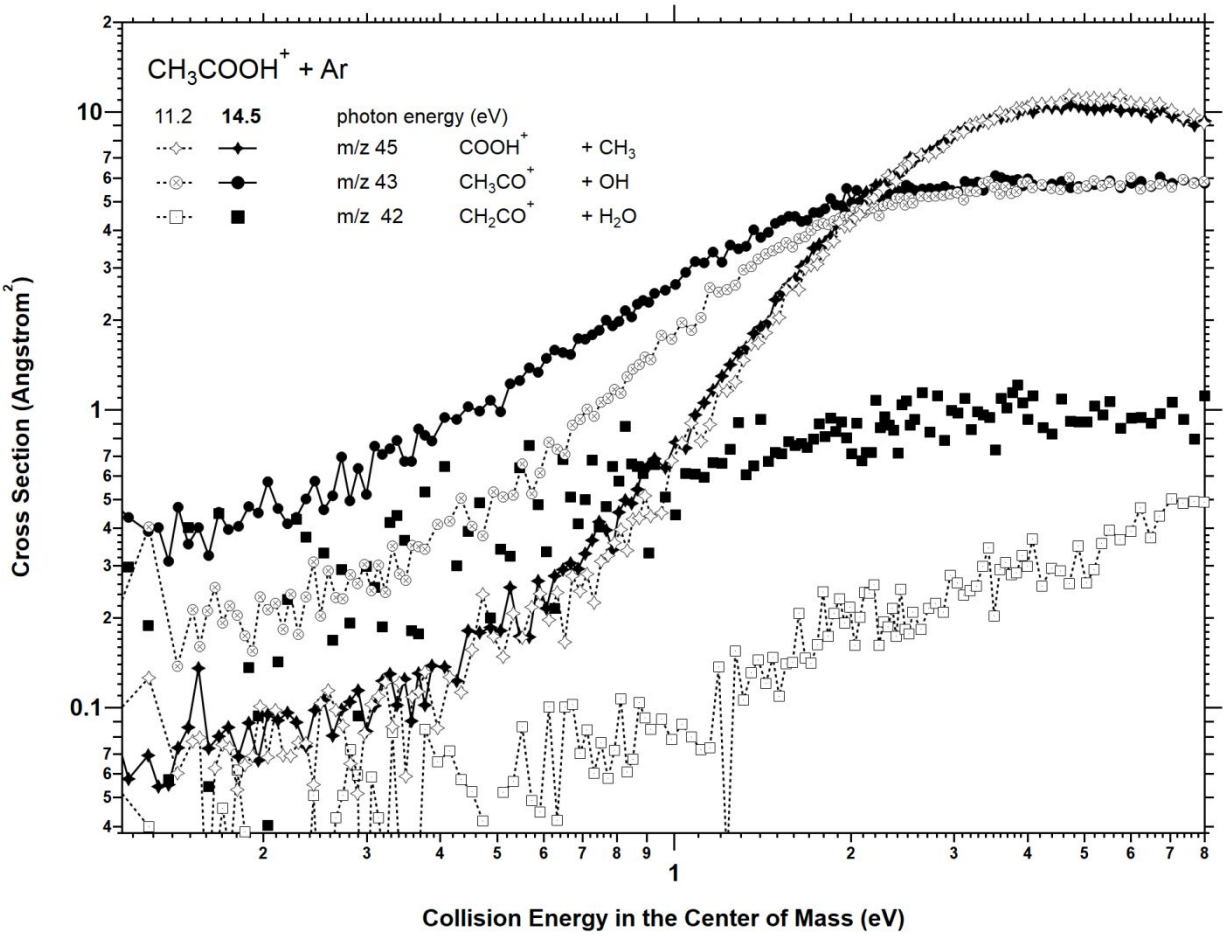

***Figure 4*: Absolute fragmentation cross sections of $CH_3COOH^{+\bullet}$ colliding with argon as a function of the center of mass collision energy. Results obtained when performing photoinization of acetic acid with 11.2 eV photons are presented with empty symbols, while results at 14.5 eV are presented with filled symbols**

$\underline{CH_3COOH^{+\bullet} + CH_3NH_2}$

The reactivity of the $CH_3COOH^{+\bullet}$ ion with CH_3NH_2 is illustrated by the mass spectrum shown in *figure 3b*. The comparison of the spectra with the reactive gas in the cell and in the chamber suggests that the following reaction would take place:

- the hydride transfer reaction:
  $CH_3COOH^{+\bullet} + CH_3NH_2 \rightarrow CH_2NH_2^+ + CH_3C(OH)_2^\bullet$ (H^-T, m/z = 30, Reaction 1a)
- a dissociative charge transfer:
  $\rightarrow CH_2NH_2^+ + H^\bullet + CH_3COOH$ (DCT, m/z = 30, Reaction 1b)
- the charge transfer reaction:
  $\rightarrow CH_3NH_2^{+\bullet} + CH_3COOH$ (CT, m/z = 31, Reaction 1c)
- the proton transfer reaction:
  $\rightarrow CH_3NH_3^+ + CH_3COO^\bullet$ (PT, m/z = 32, Reaction 1d)
- another very minor ion, key to this study, which can be associated to a peptide-like bond formation corresponds to the loss of methyl from an (unobserved) adduct:
  $\rightarrow CH_3NH_2COOH^+ + CH_3^\bullet$ (m/z = 76, Reaction 1e)
- a small amount of m/z 61 ion is also observed suggestion that the hydrogen transfer reaction also take place:
  $\rightarrow CH_2NH_2^\bullet + CH_3C(OH)_2^+$ (HT, m/z = 61, Reaction 1f)

- the ion at m/z 42, 43 and 45 were observed in our initial study and are associated to metastability and CID fragmentation processes. Alternatively, the ion at m/z 43 may be due to a further dehydratation of the $CH_3C(OH)_2^+$ ion: $CH_3C(OH)_2^+ \rightarrow H_2O + CH_3CO$ (m/z = 43, Reaction 1g)

Other minor signals are visible at m/z 40, 46 and 63 but they could not be ascribed to a direct reaction of the two reactants considered. The signals are very minor and could result from impurities present in the methylamine sample, or even to samples studied previously in the instruments which might be released from the metallic surfaces of the gas lines. The species were not further studied.

The absolute reaction cross sections for the four products at m/z 30,31,32 and 76 were measured, as well as their evolution when changing either photon or collision energy.

We show in *figure 5* the absolute cross section of the four ionic channels as a function of the photon energy. Measurements were performed at very small collision energy (0.1 eV, center of mass) in order to maximize the yield of the peptide-like bond product at m/z 76. A fake channel at m/z 73 was collected in the same conditions in order to evaluate the sensitivity of our measurements to the detector noise.

One can notice that noticeable modulation of all channels is visible in the photon energy between ionization energy (10.6 eV) and roughly 12 eV. Hence, one observes a decrease of the major CT, and concomitant increase of PT. A step is noticeable in both curves at 11.55 eV, a photon energy corresponding to the appearance of the first dissociative photoionization channel (m/z 43) as well as the maximum yield of the metastable channel at m/z 42. This indicates a modulation of the internal energy of the reactive ion that reflects into its reactivity.

The peptide-like bond formation channel is extremely faint (1/10 000 of the major channel) but it is clearly larger than the noise level, and it also exhibits some sensitivity with the photon energy. Hence, the highest cross section is recorded at the lowest photon energy, with a constant decrease reaching a plateau from 12eV and beyond. This behavior can be associated to the need for the intermediate adduct to survive for a sufficient period of time to proceed through the rearrangement leading to the product.

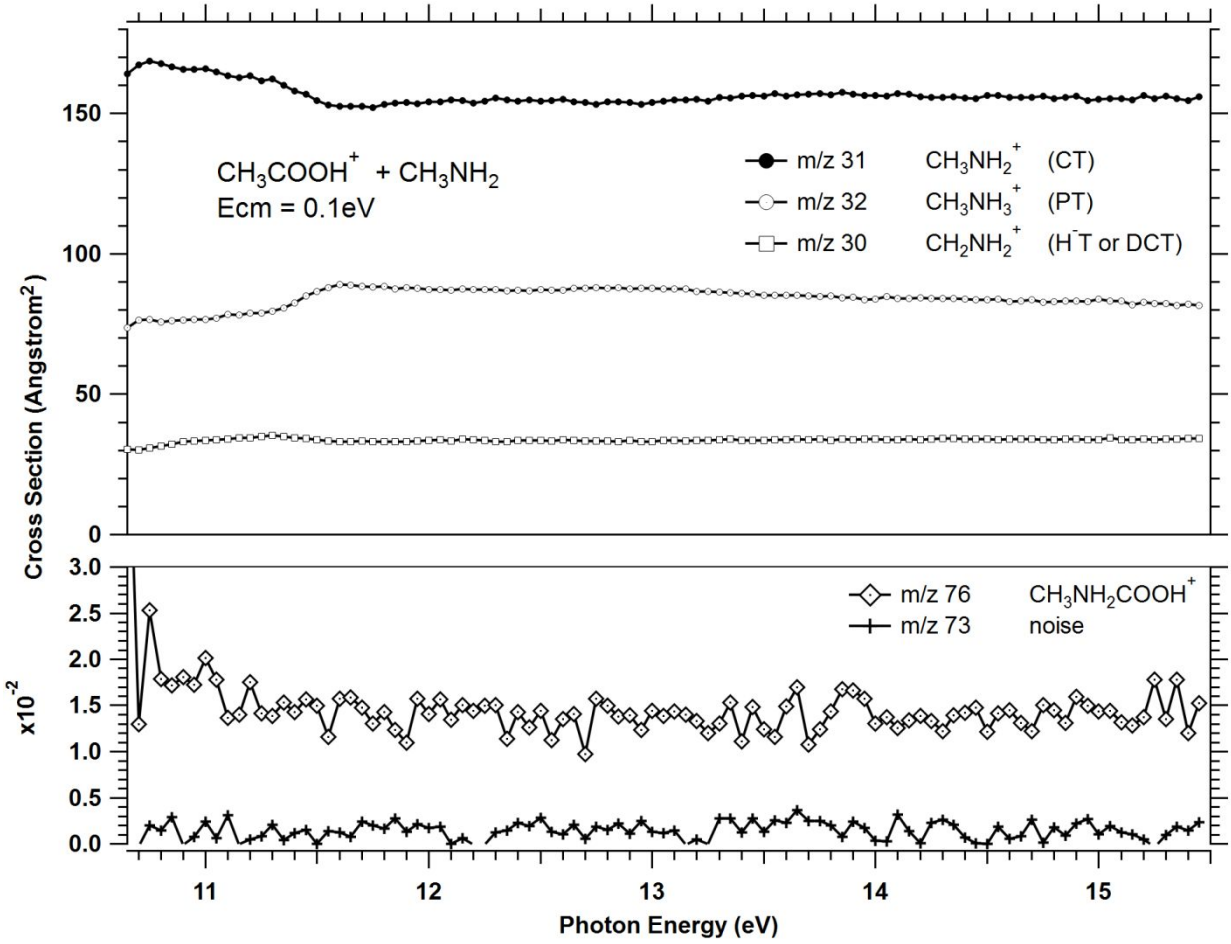

***Figure 5*: Absolute reaction cross sections of the products resulting from the reaction of $CH_3COOH^{+\bullet}$ with methylamine as a function of the photon energy used to produce the parent ion. Two scales are used in order to highlight the very minor channels. A fake channel at m/z 73 is shown to illustrate the conservative noise level associated to the measurements**

We show in *figure 6* the absolute cross section of the same ionic channels as a function of the collision energy. The measurements shown were performed at 14.5 eV, photon energy but the same acquisitions were performed at 11.2 and 12 eV and show similar trends.

An additional ionic channel corresponding at a CID process ($CH_3CO^{+\bullet}$ at m/z 43) was also recorded and exhibits an increase with collision energy, similar to the results obtained in the measurements with argon.

The cross section related to the m/z 30 ion ($CH_2NH_2^+$) is almost flat, and all other channels exhibit a decrease. It is worth mentioning that the cross section related to the m/z 31 ion, associated to the charge transfer shows a significant decrease with the collision energy (with a slope close to the $E^{-1/2}$ trend, drawn in figure 6 as a guide). This is surprising, as the usual behavior of charge transfer, due to its long range interaction, is relatively insensitive to the collision energy as has been previously observed in our apparatus.[65,66,67] In order to reconcile these observations, our hypothesis is that the m/z 31 ion is a poorly stable product of charge transfer, which dissociates to form the m/z 30 ion. Indeed, the dissociative charge transfer of $CH_3NH_2^{+\bullet}$ is known to occur for an internal energy of 1.5 eV.[68] The quantum chemical calculations presented in the following will confirm that, under our experimental conditions, the radical cation $CH_3NH_2^{+\bullet}$ formed by charge transfer dissociates to form $CH_2NH_2^+$ and $H^\bullet$. The transfer of some part of the kinetic energy imparted in the collision might be transferred in this process, leading to a comparatively increased signal at m/z 30 and a decreased signal at m/z 31.

One can observe a step between 0.3 and 0.4 eV in the cross section of the product at m/z 32 ($CH_3NH_3^+$) corresponding to proton transfer. This behaviour is well known from previous results obtained in the CERISES

instrument[65] and is the signature of secondary reactions leading to proton transfer between slowly moving ionic products and the neutral species in the cell. It is usually associated to processes occurring at large distance (such as e^-, H^+, H or H^- transfers) as those do not request an intermediate complex and do not transfer impulsion into the ionic products. Those products are therefore moving at the initial speed of the neutral species, i.e. roughly 20 meV in the center of mass. The step behaviour corresponds to the potential (0.9V) at which the ions moving backward in the instrument are repelled by a lens potential towards the detector (while they are attracted by the lens and lost at lower potentials). The amplitude of the step is informative of secondary reactions, associated to processes that do not involve an intermediate complex formation.

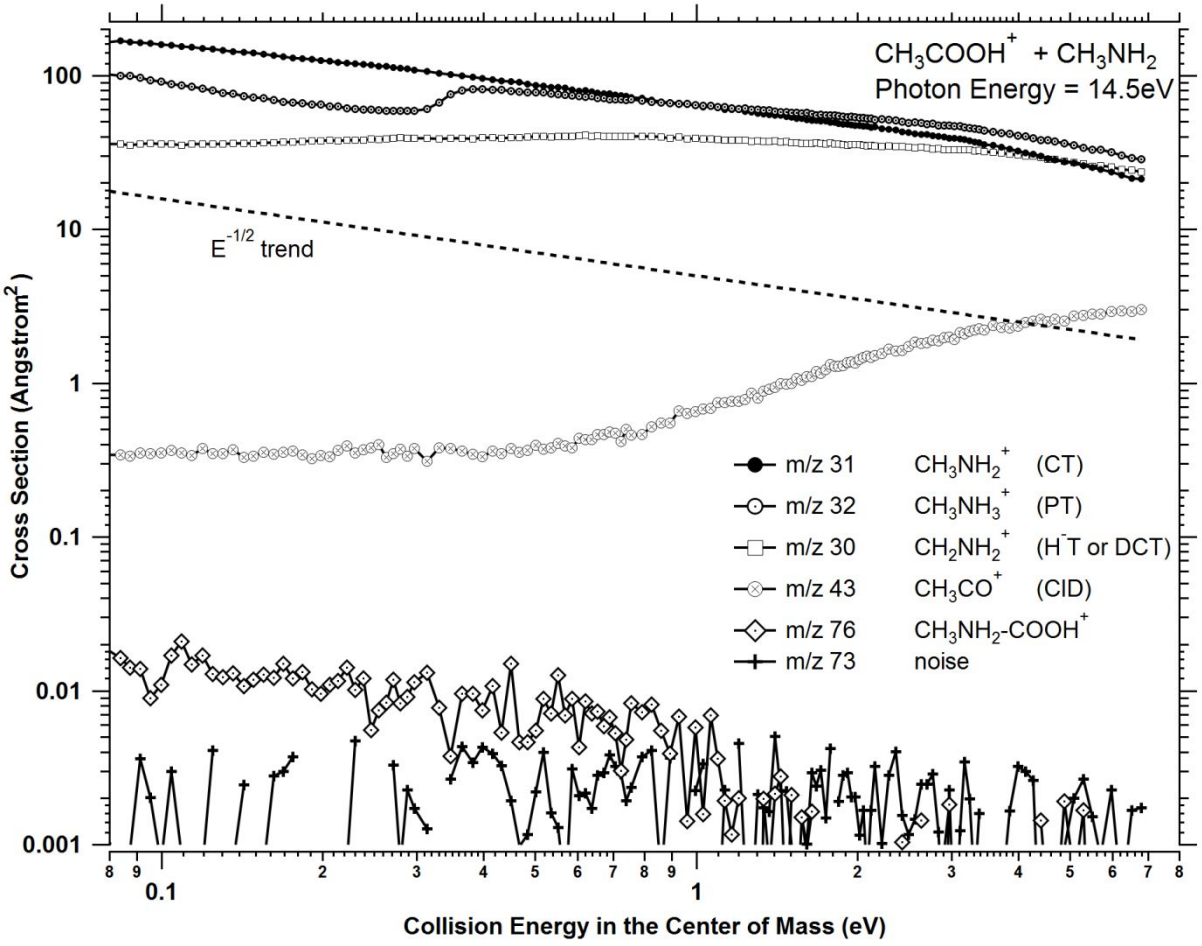

***Figure 6*: Absolute reaction cross sections of the products resulting from the reaction of $CH_3COOH^{+\bullet}$ with methylamine as a function of the collision energy. A fake channel at m/z 73 is shown to illustrate the conservative noise level associated to the measurements.**

The analysis of absolute cross sections shows that:

- the CT, DCT and PT mechanisms are clearly prevalent (between 150 and 30 Å²). This is typical when the proton affinity and/or electron affinity of the neutral partner is higher than that of the cation radical reagent,
- the effective ion-forming cross sections at m/z 76 is very small, but these ions are clearly evidenced above the background and do therefore correspond to reaction products.

The reaction paths corresponding to these different processes were investigated using DFT-D calculations. From a theoretical point of view, we have identified the different stationary points corresponding to these

processes. Two possible structures were found for the $C_2H_5O_2^{\bullet}$ radical formed from the hydride transfer (See Figure 7 and Supplementary Data). The values presented in *figure 7* takes into account the ZPE correction, and the frequency calculations allowed us to verify the nature (minimum or transition state) of the stationary points. (The minor 1f and 1g reaction pathways are presented in Supplementary Data).

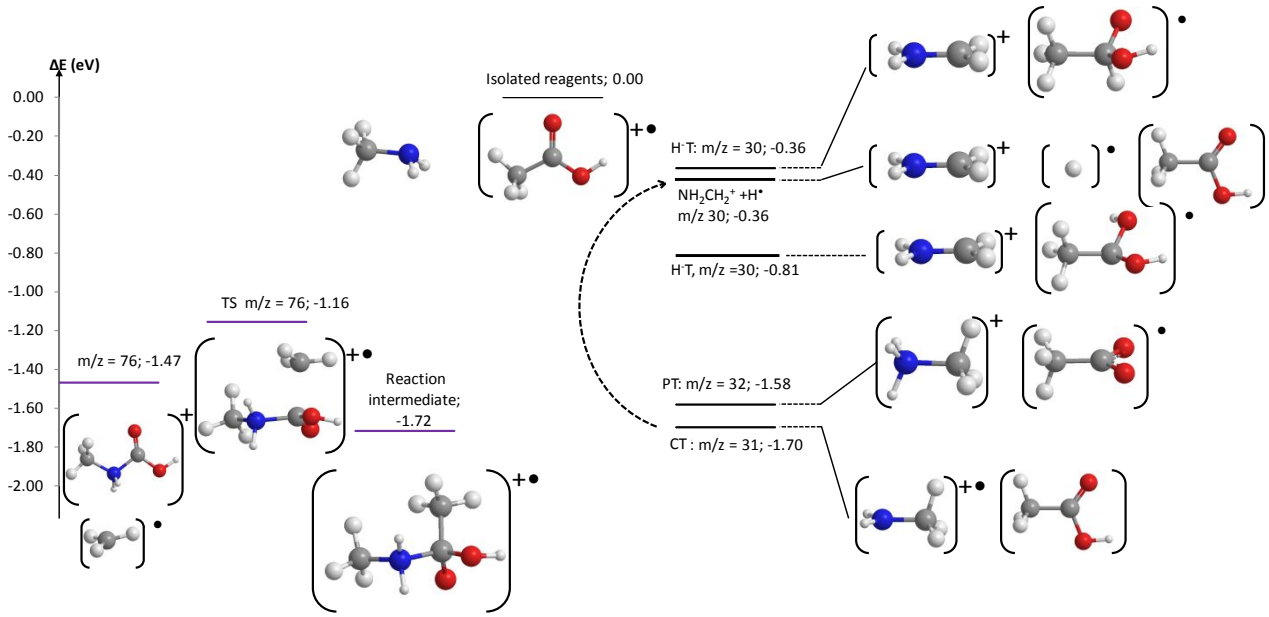

***Figure 7*: Identification of stationary states on the potential energy surface for the reaction between $CH_3COOH^{+\bullet}$ and CH_3NH_2. (The minor 1f and 1g reaction pathways are presented in Supplementary Data)**

The mechanisms of proton transfer, charge transfer and hydride transfer are calculated to be exothermic.

As pointed out in the analysis of the cross-sections presented in *figure 6*, we have also considered the subsequent charge transfer dissociation of $CH_3NH_2^{+\bullet}$ (m/z 31) into $CH_2NH_2^{+}$ (m/z 30) and $H^{\bullet}$. As the internal energy that can be stored in the $CH_3NH_2^{+\bullet}$ CT product is higher than the energy needed to fragment it with a H loss, the DCT channel is indeed energetically feasible. This fragmentation allows to explain the behaviour observed in *figure 6*.

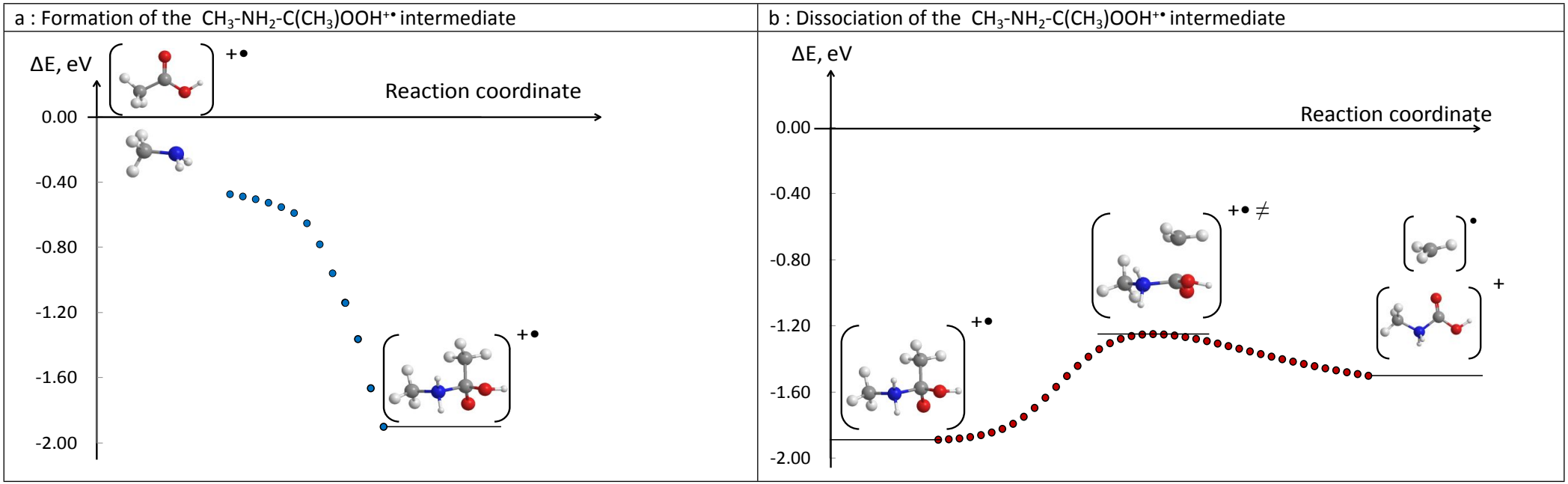

***Figure 8**: Identification of a two-step mechanism to explain the formation of the C(O)-N bond and production of the CH_3-NH_2-$COOH^+$ cation with concomitant loss of the methyl radical from the reaction of the $CH_3COOH^{+\bullet}$ radical cation and methylamine.*

For the reaction leading to the formation of the ion at m/z 76, a two-step mechanism can be proposed, with a simple association mechanism of the two species (*figure 8*). From this reaction intermediate, a transition state leads to the formation of the product CH_3-NH_2-$COOH^+$ with the concomitant loss of the CH_3 radical. This mechanism was confirmed by partially relaxed scan calculations (for the formation of the reaction intermediate from the reagents, *figure 8*,a) and IRC, for the part of the mechanism leading to the reaction products from the reaction intermediate, *figure 8*,b). Note that these potential energy surfaces do not take into account the ZPE correction, hence the slight discrepancy between the values in *figure 7* and in *figure 8*.

Thus, from the parent ion $CH_3COOH^{+\bullet}$ taken in its fundamental state, a "C(O)-N bond-forming reaction" is observed. The effective cross section of this reaction is about 10,000 times smaller than that of the PT, CT and H^-T processes, but quantum chemistry calculations confirm that the parent ion $CH_3COOH^{+\bullet}$ taken in its ground state can react with CH_3NH_2 to form CH_3-NH_2-$COOH^+$ with the concomitant loss of the $CH_3^\bullet$ radical. This is not formally a peptide-bond, but rather the formation of a carbamate cation.

We aimed at finding out if another "C(O)-N bond-forming reaction" could take place with the concomitant loss of a water molecule, to get closer to the typical peptide C(O)-N bond-forming processes. This is why we focused on the reactivity of the fragment ion at m/z=45 $COOH^+$, the only one that may lead to this type of process among the most abundant ions formed in the dissociative photoionization of CH_3COOH.

$COOH^+ + CH_3NH_2$

The dissociative photoionization of acetic acid leads to the formation of the $COOH^+$ cation (m/z 45). From the parent ion $CH_3COOH^{+\bullet}$, the $COOH^+$ fragment ion was selected in mass with the quadrupole I in order to introduce it into the reaction cell and study its reactivity with CH_3NH_2. The mass spectrum obtained at a photon energy of 14.5 eV is presented in *figure 9,* a. The formation of ions at m/z 30, 32, 46, 58 and 60 is observed. Compared to what was observed in the case of the reaction of $CH_3COOH^{+\bullet}$ with CH_3NH_2, one can notice the absence of the ion at m/z 31. Hence the faint signal located between m/z 30 and 32 can be ascribed to the ^{13}C isotope abundance present in methylamine.

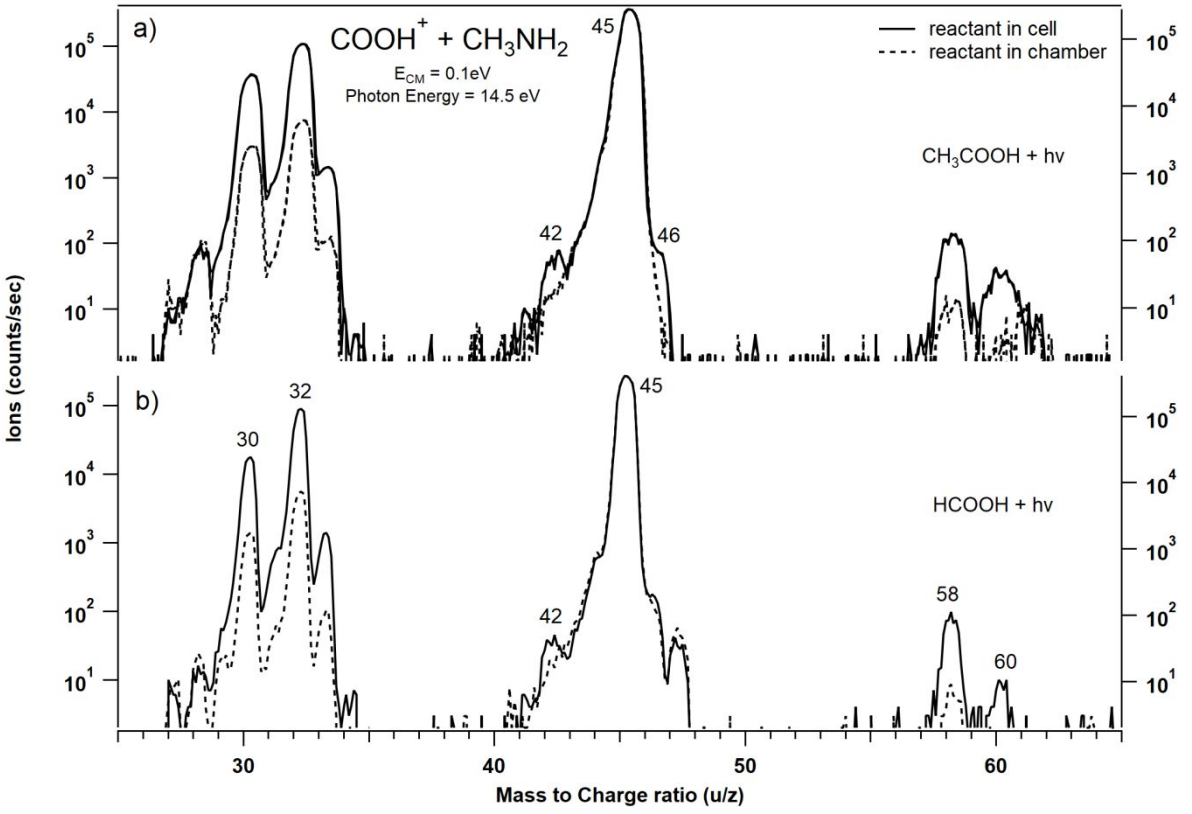

***Figure 9*: Mass spectra of ions produced in the reaction of $COOH^+$ and methylamine, with the m/z 45 parent ion prepared through dissociative photoionization at 14.5 eV photon energy of (a) acetic acid or (b) formic acid. In each case, two spectra are shown with either the methylamine reactant gas introduced in the cell (continuous line, left scale) or in the chamber surrounding the cell (dashed line, right scale).**

The comparison of the spectra with the reactive gas in the cell and in the chamber suggests that the following reaction would take place:

- the hydride transfer reaction:
  $CH_3NH_2 + COOH^+ \rightarrow CH_2NH_2^+ + HCOOH$ (H^-T, m/z = 30, Reaction 2a)

- the proton transfer reaction:
  $\rightarrow CH_3NH_3^+ + CO_2$ (PT, m/z = 32, Reaction 2b)

- the dissociative proton transfer:
  $\rightarrow CH_2NH_2^+ + H_2 + CO_2$ (DPT, m/z = 30, Reaction 2c)

- the C(O)-N bond formation reaction:
  $\rightarrow CH_3NHCO^+ + H_2O$ (CN, m/z = 58, Reaction 2d)

- other minor product ions are observed at m/z 46 and 60.

As a comparison, we also investigated the reaction of CH_3NH_2 with $COOH^+$ ions formed by dissociative photoionization of another precursor, the formic acid, HCOOH. *Figure 9,* b shows very similar ionic products obtained when using formic acid as precursor of the $COOH^+$ ion.

*Figure 10,*a shows the absolute cross sections of the reaction of the $COOH^+$ fragment ion from acetic acid with methylamine as a function of the energy of the photons used for ionization. As in the previous case, the H^-T and PT mechanisms are highly dominant. Moreover, these results show that:

- the appearance energy of the $COOH^+$ fragment ion is $EA_{exp}^{45} \approx 12.1\ eV$ (see Fig. 1)

- the two major products appear at the first energies probed, as do the minor m/z = 58 product within uncertainties of its low signal.

This allows one to consider that the reactions take place already from the reagents taken in their fundamental state.

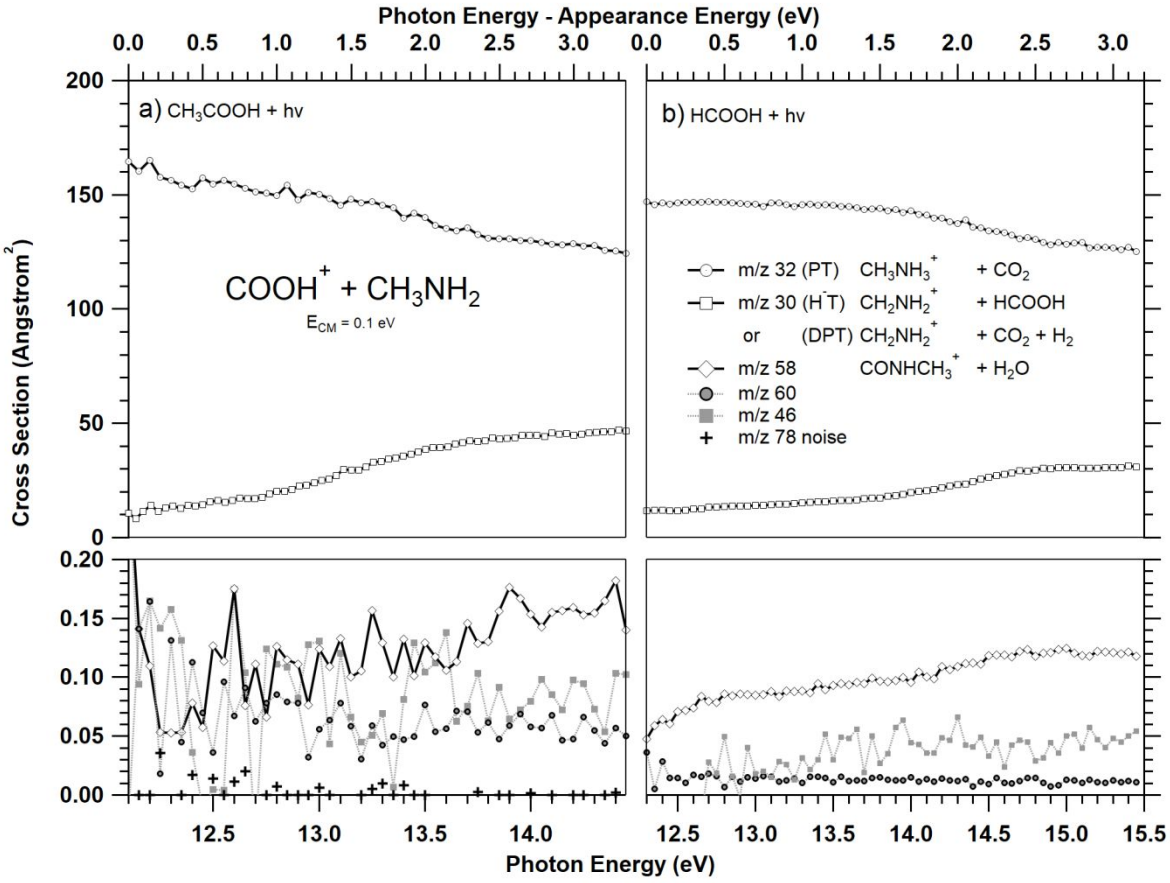

***Figure 10*: Absolute reaction cross sections for the various product channels in the reaction of $COOH^+$ with methylamine as a function of the photon energy used to produce the parent ion. Two horizontal scales are used to differentiate $COOH^+$ reactant ion produced from a) acetic or b) formic acid. Two vertical scales are used in order to highlight the minor channels. A fake channel at m/z 78 is shown to illustrate the conservative noise level associated to the measurements**

Figure 10 b shows the absolute cross sections of the reaction of the $COOH^+$ fragment ion from formic acid with methylamine as a function of the energy of the photons used for ionization. These results show that:

- the appearance energy of the $COOH^+$ fragment ion is $EA_{exp}^{45} = 12.3 \pm 0.05eV$ (see Fig. 2)
- the appearance energies of all the m/z = 30, 32 and 58 products of the reaction are close to this value.

Thus, the $COOH^+$ ion taken in its fundamental electronic state can react with neutral CH_3NH_2 to form the $CH_2NH_2^+$, $CH_3NH_3^+$ and CH_3NHCO^+ products.

It is worth mentioning that secondary reactions involving methylamine radical cation could also lead to the formation of ions NH_2CH_2-$CH_2NH_2^{+\bullet}$ and NH_2CH=$CHNH_2^{+\bullet}$ with m/z ratios of 60 and 58, respectively:

$CH_3NH_2^{+\bullet} + CH_3NH_2 \rightarrow NH_2CH_2$-$CH_2NH_2^{+\bullet}$ (or $[(NH_2CH_2)_2]^{+\bullet}$, m/z 60) $+ H_2$

$\rightarrow NH_2CH$=$CHNH_2^{+\bullet}$ (m/z 58) $+ 2\ H_2$

However, we showed that the $CH_3NH_2^{+\bullet}$ species could not be formed in the case of the reaction of $COOH^+$ with CH_3NH_2, so these processes can be eliminated.. Moreover, the ions at m/z 58 and either 30, 31 or 32 do not have a similar behavior, which makes it possible to eliminate this secondary reaction process (the theoretical data are nonetheless provided in SI).

Furthermore, *figure 10* allows comparison of the reactivity with CH_3NH_2 of $COOH^+$ ions coming either from CH_3COOH or from HCOOH. Notable differences in the cross section of the ions at m/z 30 and 32 can be observed, depending on the photon energy and nature of the ionized precursor:

- the cross section for the formation of the $CH_3NH_3^+$ ion (m/z 32) at threshold is lower in the reaction of the $COOH^+$ ion produced from formic acid than from acetic acid,
- conversely, the cross section for the formation of the $CH_2NH_2^+$ ion (m/z 30) at threshold is higher in the reaction of the $COOH^+$ ion produced from formic acid than from acetic acid.
- In both cases, there is an important (times fives) increase of the cross section of the $CH_2NH_2^+$ product and a concomitant decrease in the cross section of the $CH_3NH_3^+$ product with photon energy.
- furthermore, the amplitude of the variations for both cross sections with photon energy is larger in the case of the reaction of the $COOH^+$ ion formed from CH_3COOH.

These results are in favor of our description of the channel products at m/z 32 and 30 as being the result of proton transfer and dissociative proton transfer process. One can therefore assume that some excess of energy will lead to a transfer of cross section from one channel to the other, as is observed here. These results further underline a strong sensitivity of the reactive channels to the internal energy of the $COOH^+$ ions, and the ability to alter significantly the $COOH^+$ internal energy when changing the photon energy, though there is here no control of the amount of energy released in the photoelectron nor in the neutral partner (either $CH3^\bullet$ or $H^\bullet$). The amplitude of the variation can be correlated to the presence of the second excited state, described in figures 1 and 2 (states 2a" and 9a' for acetic and formic acid, respectively). Hence, as was noted, the yield of $COOH^+$ ions exhibit a stronger increase (6 to 1) for acetic acid than for formic acid (1 to 1) when this state is produced. One can therefore assume that the larger amount of excited precursor will induce a larger amount of excited $COOH^+$ reactant, and therefore produce more contrasted results, as in observed in figure 10. The most intriguing result is the different behaviour at threshold, which suggests that the $COOH^+$ ions are formed in different internal energy states, depending on the neutral partner that is released in the dissociative photoionization process. One can note here that in the case of acetic acid, the neutral partner is $CH3^\bullet$, while it is $H^\bullet$ in formic acid. This corresponds to the breakage of a C-C bond in one case and a C-H bond in the other case. The latter being a stronger bond, one can expect the need to produce a population of precursor with comparatively larger internal energy to produce the $COOH^+$ fragment in the case of formic acid, that would induce the observed phenomenon.

The cross section for the production of m/z 58 product related to the peptide-like bond formation exhibit also some sensitivity to the photon energy. Hence, for both precursors, there is a slight increase above threshold and a second increase correlated to the abovementioned excited state production. An excess of internal energy in the reactants is not mandatory, but beneficial to its formation.

Finally, the cross sections presented in *figure 10* confirm that the ions at m/z 46 and 60 are due to reactions with residual compounds as their evolution with the photon energy exhibit a large variability in their intensity between the two experimental sets, most probably related to their

transient behavior, with a lower relative intensity when performing measurements at a later stage of the experimental session.

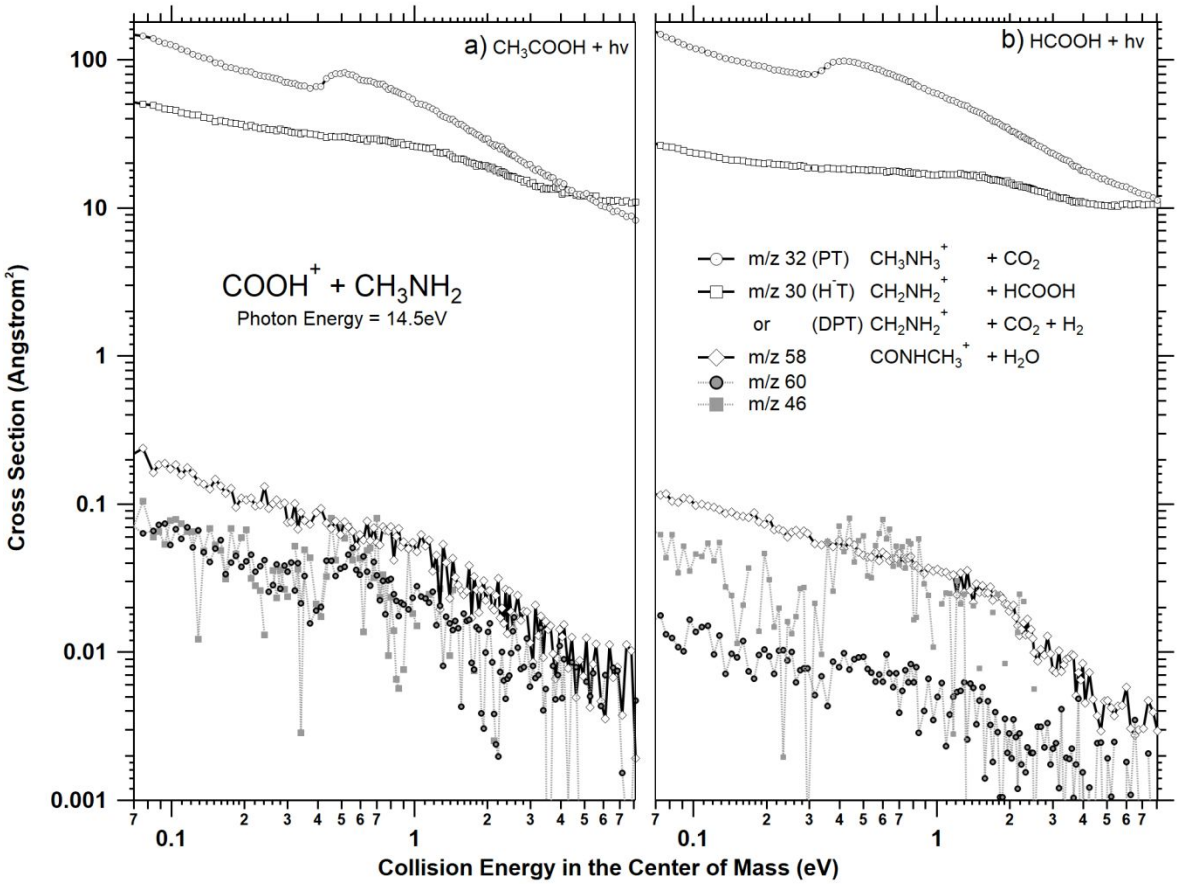

***Figure 11*: Absolute reaction cross sections of the various product channels in the reaction of $COOH^+$ with methylamine as a function of the collision energy. Two horizontal scales are used to differentiate $COOH^+$ reactant ion produced from a) acetic or b) formic acid.**

Figure 11 shows the absolute cross sections of the reaction of the $COOH^+$ fragment ion from acetic and formic acid with methylamine as a function of the collision energy. Similarly to results obtained with the $CH_3COOH^{+\bullet}$ precursor (shown in figure 6), a step function is observed in the PT channel, signature of some amount of secondary reactions. As discussed earlier, the products at m/z 30 and 32 exhibit a coupled behaviour, with comparatively increased cross section for the m/z 30 ion when collision energy is increased. Furthermore, the hypothesis that $COOH^+$ ion brings more energy in the reaction when using acetic acid as precursor is clearly confirmed, as the two partners have closer cross sections at threshold and m/z 30 even surpass m/z 32 at 8 eV collision energy.

The absolute cross section trend for the formation of a peptide-like bond exhibit a $E^{-1/2}$ trend, signature of a complex formation, and maximum reactivity at very low collision energy. However, this reaction is 100 to 1,000 times less efficient than the proton and dissociative proton transfer processes.

Finally, the reaction pathways deduced from experimental observations (Reactions 2a - 2d) were investigated using DFT-D calculations. It is worth mentioning that the formation of the ion at m/z 31, $CH_3NH_2^{+\bullet}$, has not been observed. An attempt has been made to understand why, considering it as one of the possible processes.

Several structures were investigated for the ions at m/z 60 and 46, as well as for the corresponding neutral fragments, but no exothermic pathway could be identified. Since these fragments are very minor, they may be products formed after reaction with residual gases present in the reaction chamber.

The stationary points that could be identified on the potential energy surface for the reaction between CH_3NH_2 and $COOH^+$ are shown in *figure 12*. All energies given in this figure take into account the ZPE correction and have been calculated at LC-ωPBE/6-311++G(d,p) + GD3BJ. The nature (TS or local minimum) of the stationary points has been verified by frequency calculations.

It is worth mentioning that the calculations suggest that the $COOH^+$ fragment ion formed by dissociative photoionization of acetic acid and formic acid have the same structure. They may however differ in their internal energies, which could directly affect their reactivity.

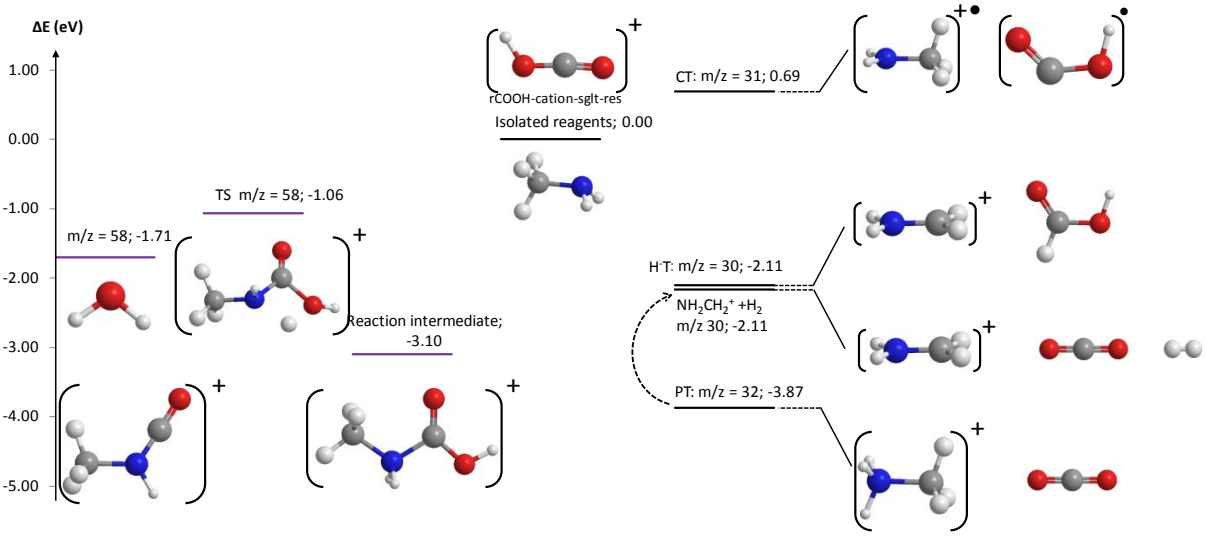

***Figure 12*: Identification of stationary states on the potential energy surface for the reaction between the $COOH^+$ ion and CH_3NH_2.**

A basic energy analysis provides an understanding of the absence of ion formation at m/z 31: the charge transfer, which would lead to the formation of a radical and a cation radical from a cation and a neutral species, is calculated as being endothermic.

As in the case of the formation of the ion at m/z 76 from the $CH_3COOH^{+\bullet}$ and CH_3NH_2 species, a two-step mechanism could be identified for the formation of the ion at m/z 58 from the $COOH^+$ and CH_3NH_2 reagents taken in their fundamental state (*figure 13*).

A : Formation of the CH_3-NH_2-$COOH^+$ reaction intermediate	B : Dissociation of the CH_3-NH_2-COOH reaction intermediate, with the concomitant loss of one water molecule

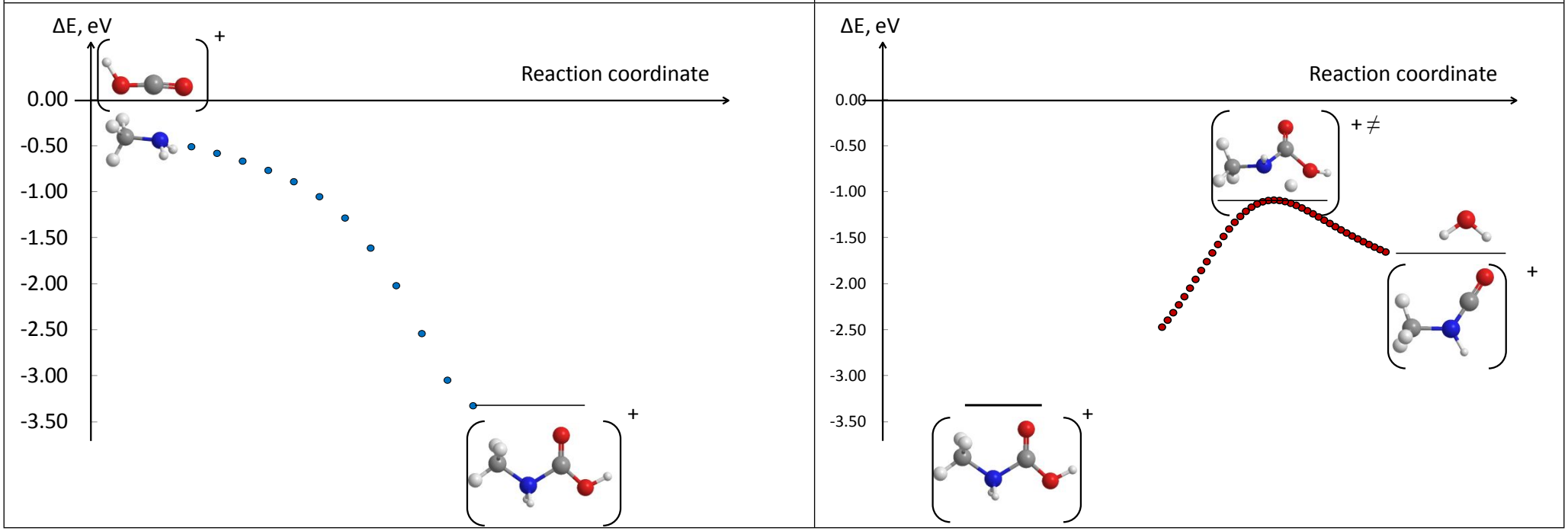

***Figure 13*: Identification of a two-step mechanism to explain the formation of the C(O)-N bond and the production of the CH_3-NH-CO^+ cation with concomitant loss of a water molecule from the $COOH^+$ cation and methylamine.**

- the formation of the CH_3-NH_2-$COOH^+$ intermediate, following an inverse process of the expected simple cleavage of the C(O)-N bond in the CH_3-NH_2-$COOH^+$: no energy barrier is associated with this process. The formation of this intermediate is accompanied by a strong stabilization of the system (ΔE = 3.10 eV, *figure 13* a),
- a rearrangement, including the migration of a hydrogen atom from the nitrogen atom to the oxygen atom, leading to the loss of water. The energy barrier associated with this process is ΔE = 2.04 eV (*figure 13* b), thus below the entrance channel energy.

IV. Discussion

In this work, we have identified two reactions leading to the formation of a peptide C(O)-N bond between methylamine and a cation or a radical cation taken in their fundamental state:

- the $CH_3NHCOOH^+$ (m/z 76) formation with the concomitant loss of the $CH_3^\bullet$ radical from the reaction of the $CH_3COOH^{+\bullet}$ radical cation produced by photoionization of acetic acid,
- the CH_3NHCO^+ formation with the concomitant loss of one water molecule from the reaction of the $HCOO^+$ cation produced by dissociative photoionization of acetic and formic acid.

In both cases, theoretical studies have revealed a two-step reaction mechanism: i) the formation of a reaction intermediate without an energy barrier, following a process that is the reverse of that of the simple cleavage of a chemical bond, and ii) a rearrangement within this reaction intermediate, leading to the loss of a radical or molecular species. No energy excess seems necessary for these processes, which are of major interest for prebiotic chemistry, to occur.

This result is very different from what is calculated in the case of the reaction between neutral CH_3COOH and CH_3NH_2 :[30] the photoionization of the acid partner greatly favors the reaction, from a thermodynamic point of view. This is somewhat similar to the results recently reported by Darla and Sitha on the theoretical study of the reaction between NH_3 and CO, NH_3^+ and CO and NH_3 and CO^+:[69] the mechanism of formation of the C(O)-N bond is clearly favored from a thermodynamic point of view in the case of NH_3 and CO^+ compared to the other two cases. It is also worth underlying that another possible C(O)-N bond forming reaction that could occur in the interstellar medium was recently evidenced from acrylonitrile and ammonia.[70]

Furthermore, it should be noted that ions at m/z 76 were also observed from the reaction between NH_3OH^+ and CH_3COOH,[71] as well as in infrared assisted synthesis of prebiotic glycine.[72] Further studies on the formation of such prebiotic ions would be of great interest.

V. Conclusion

Effects of photon and collision energy on the various reaction channels have been recorded and constitute a coherent set of information, showing important internal energy effects, related to the presence of excited states in the considered energy range. The particular case of producing $COOH^+$ from two different precursors allowed to identify specific behaviour, related to the probable larger internal energy content for the ion produced by dissociative photoionization from acetic acid than from formic acid.

The C(O)-N bond-forming processes herein evidenced proved to be possible, but much less efficient than the non-specific mechanisms of proton, hydride and charge transfer and associated dissociative processes between methylamine and the mass-selected ion. Thus, it seems essential to further study this kind of reactions in order to determine whether, in some cases, peptide-like C(O)-N bond formation reactions between simple precursors present in the interstellar medium could be more efficient and lead to the formation of prebiotic species. In particular, the presence of a few water molecules could greatly promote these processes, as has been demonstrated experimentally by G. van der Rest et al.[73,74] and theoretically by G. Bouchoux et al.,[29] for example. This is why we plan to couple the CERISES set-up with a supersonic jet on the DESIRS beamline of the SOLEIL synchrotron, to study the reaction of the $\{CH_3COOH^{+\bullet}, (H_2O)_n\}$ and $\{COOH^+, (H_2O)_n\}$ complexes with methylamine, with $1 \leq n \leq 4$.

Acknowledgments

We thank the DESIRS beamline team, for assistance during the synchrotron measurements. We are most grateful to SOLEIL for financial support and to the technical staff for running the facility during the project n◦20190680.

Supporting Information.

Determination of the experimental lifetime for the metastable process leading to m/z 42 ion in the dissociative photoionization of acetic acid.

Optimized geometries of the species at the LC-wPBE/6-311++G(d,p) level of theory with their energies (including ZPE corrections).

For Table of Contents Only

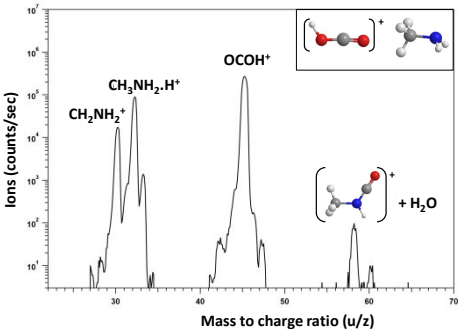

References

[1] Herbst E., Dishoeck E. Complex Interstellar Organic Molecules. Annu. Rev. Astron. Astrophys. 2009;47:427. doi: 10.1146/annurev-astro-082708-101654

[2] Hollis J.M., Vogel S.N., Snyder L.E., Jewell P.R., Lovas F.J. Interstellar glycolaldehyde: The first sugar. Astrophys. J. 2000;540:L107

[3] Hollis, J. M., Jewell, P. R., Lovas, F. J., & Remijan, A. (2004). Green bank telescope observations of interstellar glycolaldehyde: low-temperature sugar. *The Astrophysical Journal Letters*, *613*(1), L45.

[4] Fourikis, N., Takagi, K., & Morimoto, M. (1974). Detection of Interstellar Methylamine by its 2_ {02}-> 1_ {10} A_ {a^{-}} State Transition. *The Astrophysical Journal*, *191*, L139.

[5] Rivilla, V. M., Martín-Pintado, J., Jiménez-Serra, I., Martín, S., Rodríguez-Almeida, L. F., Requena-Torres, M. A., Rico-Villas, F., Zeng, S., & Briones, C. (2020). Prebiotic precursors of the primordial RNA world in space: Detection of NH2OH. *The Astrophysical Journal Letters*, *899*(2), L28.

[6] Glavin, D. P., Dworkin, J. P., & Sandford, S. A. (2008). Detection of cometary amines in samples returned by Stardust. *Meteoritics & Planetary Science*, *43*(1-2), 399-413.

[7] Elsila, J. E., Glavin, D. P., & Dworkin, J. P. (2009). Cometary glycine detected in samples returned by Stardust. *Meteoritics & Planetary Science*, *44*(9), 1323-1330.

[8] Altwegg, K., Balsiger, H., Bar-Nun, A., Berthelier, J. J., Bieler, A., Bochsler, P., Briois, C., Calmonte, U., Combi, M.R., Cottin, H. et al.(2016). Prebiotic chemicals—amino acid and phosphorus—in the coma of comet 67P/Churyumov-Gerasimenko. *Science advances*, *2*(5), e1600285.

[9] Zuckerman, B., Ball, J. A., & Gottlieb, C. A. (1971). Microwave detection of interstellar formic acid. *The Astrophysical Journal*, *163*, L41.

[10] Mehringer, D. M., Snyder, L. E., Miao, Y., & Lovas, F. J. (1997). Detection and confirmation of interstellar acetic acid. *The Astrophysical Journal Letters*, *480*(1), L71.

[11] Baiano, C., Lupi, J., Tasinato, N., Puzzarini, C., & Barone, V. (2020). The role of state-of-the-art quantum-chemical calculations in astrochemistry: formation route and spectroscopy of ethanimine as a paradigmatic case. *Molecules*, *25*(12), 2873.

[12] Ioppolo, S., Fedoseev, G., Chuang, K. J., Cuppen, H. M., Clements, A. R., Jin, M., Garrod, R. T., Qasim, D., Kofman, V., van Dishoeck, E. F. et al. (2020). A non-energetic mechanism for glycine formation in the interstellar medium. *Nature Astronomy*, 1-9.

[13] Tan, X. F., Zhang, L., & Long, B. (2020). New mechanistic pathways for the formation of organosulfates catalyzed by ammonia and carbinolamine formation catalyzed by sulfuric acid in the atmosphere. *Physical Chemistry Chemical Physics*, *22*(16), 8800-8807.

[14] Liu, J. Y., Long, Z. W., Mitchell, E., & Long, B. (2021). New Mechanistic Pathways for the Reactions of Formaldehyde with Formic Acid Catalyzed by Sulfuric Acid and Formaldehyde with Sulfuric Acid Catalyzed by Formic Acid: Formation of Potential Secondary Organic Aerosol Precursors. *ACS Earth Space Chem.* 2021, 5, 6, 1363–1372

[15] Dong, Z. G., Xu, F., & Long, B. (2018). The energetics and kinetics of the CH3CHO+(CH3) 2NH/CH3NH2 reactions catalyzed by a single water molecule in the atmosphere. *Computational and Theoretical Chemistry*, *1140*, 7-13.

[16] Galloway, M. M., Powelson, M. H., Sedehi, N., Wood, S. E., Millage, K. D., Kononenko, J. A., Rynaski, A. D. & De Haan, D. O. (2014). Secondary organic aerosol formation during evaporation of droplets

containing atmospheric aldehydes, amines, and ammonium sulfate. *Environmental science & technology*, *48*(24), 14417-14425.

[17] Dong, Z. G., Xu, F., Mitchell, E., & Long, B. (2021). Trifluoroacetaldehyde aminolysis catalyzed by a single water molecule: An important sink pathway for trifluoroacetaldehyde and a potential pathway for secondary organic aerosol growth. *Atmospheric Environment*, *249*, 118242.

[18] Colzi, L., Rivilla, V. M., Beltrán, M. T., Jiménez-Serra, I., Mininni, C., Melosso, M., Cesaroni, R., Fontani, F., Lorenzani, A., Sanchez-Monge , A. et al. (2021). The GUAPOS project II. A comprehensive study of peptide-like bond molecules. *Astronomy & Astrophysics*, *653*, A129.

[19] Georgelin, T., Jaber, M., Bazzi, H., & Lambert, J. F. (2013). Formation of activated biomolecules by condensation on mineral surfaces–a comparison of peptide bond formation and phosphate condensation. *Origins of Life and Evolution of Biospheres*, *43*(4), 429-443.

[20] Rimola, A., Tosoni, S., Sodupe, M., & Ugliengo, P. (2006). Does Silica Surface Catalyse Peptide Bond Formation? New Insights from First-Principles Calculations. *ChemPhysChem*, *7*(1), 157-163

[21] Rimola, A., Sodupe, M., & Ugliengo, P. (2019). Role of mineral surfaces in prebiotic chemical evolution. In silico quantum mechanical studies. *Life*, *9*(1), 10.

[22] Georgelin, T., Akouche, M., Jaber, M., Sakhno, Y., Matheron, L., Fournier, F., Méthivier, C., Martra, G. & Lambert, J. F. (2017). Iron (III) oxide nanoparticles as catalysts for the formation of linear glycine peptides. *European Journal of Inorganic Chemistry*, *2017*(1), 198-211.

[23] Tielens, F., Gierada, M., Handzlik, J., & Calatayud, M. (2020). Characterization of amorphous silica based catalysts using DFT computational methods. *Catalysis Today*, *354*, 3-18.

[24] Pantaleone, S., Ugliengo, P., Sodupe, M., & Rimola, A. (2018). When the surface matters: prebiotic peptide-bond formation on the TiO2 (101) anatase surface through periodic DFT-D2 simulations. *Chem. Eur. J*, *24*, 16292-16301.

[25] Rufino, V. C., & Pliego Jr, J. R. (2020). The role of carboxylic acid impurity in the mechanism of the formation of aldimines in aprotic solvents. *Computational and Theoretical Chemistry*, *1191*, 113053.

[26] Louie, M. K., Francisco, J. S., Verdicchio, M., Klippenstein, S. J., & Sinha, A. (2016). Dimethylamine addition to formaldehyde catalyzed by a single water molecule: a facile route for atmospheric carbinolamine formation and potential promoter of aerosol growth. *The Journal of Physical Chemistry A*, *120*(9), 1358-1368.

[27] Dong, Z. G., Xu, F., & Long, B. (2018). The energetics and kinetics of the CH3CHO+(CH3) 2NH/CH3NH2 reactions catalyzed by a single water molecule in the atmosphere. *Computational and Theoretical Chemistry*, *1140*, 7-13.

[28] Perez, J. E., Kumar, M., Francisco, J. S., & Sinha, A. (2017). Oxygenate-Induced Tuning of Aldehyde-Amine Reactivity and Its Atmospheric Implications. *The Journal of Physical Chemistry A*, *121*(5), 1022-1031.

[29] Riffet, V., Frison, G., & Bouchoux, G. (2018). Quantum-chemical modeling of the first steps of the Strecker synthesis: from the gas-phase to water solvation. *The Journal of Physical Chemistry A*, *122*(6), 1643-1657.

[30] Zins E.L., Derbali I., Alikhani M.E., Alcaraz C., Romanzin C., Thissen R. On the relevance of the molecular electronic potential for the study of micro-hydration and its impact on the formation of a peptid bond, Under Preparation.

[31] Alcaraz, C., Nicolas, C., Thissen, R., Žabka, J., & Dutuit, O. (2004). 15N+ + CD4 and O+ + 13CO2 state-selected ion-molecule reactions relevant to the chemistry of planetary ionospheres. *J. Phys. Chem. A* 108, 9998–10009.

[32] Cunha de Miranda, B., Romanzin, C., Chefdeville, S., Vuitton, V., Žabka, J., Polášek, M., & Alcaraz, C. (2015). Reactions of state-selected atomic oxygen ions O+(4S, 2D, 2P) with methane. *J. Phys. Chem. A* 119, 6082–6098.

[33] Nahon, L., de Oliveira, N., Garcia, G. A., Gil, J.-F., Pilette, B., Marcouillé, O, Lagarde, B., & Polack, F. (2012). DESIRS: a state-of-the-art VUV beamline featuring high resolution and variable polarization for spectroscopy and dichroism at SOLEIL. J. Synchrotron Rad. 19, 508–520.

[34] Mercier, B., Compin, M., Prevost, C., Bellec, G., Thissen, R., Dutuit, O., & Nahon, L. (2000). Experimental and theoretical study of a differentially pumped absorption gas cell used as a low energy-pass filter in the vacuum ultraviolet photon energy range. *Journal of Vacuum Science & Technology A: Vacuum, Surfaces, and Films*, 18(5), 2533-2541.

[35] Minnhagen, L. (1973). Spectrum and the energy levels of neutral argon, Ar I. *JOSA*, *63*(10), 1185-1198.

[36] *NIST Atomic Spectra Database*. Available: http://physics.nist.gov/asd

[37] Gaussian 09, Revision D.01, M. J. Frisch, G. W. Trucks, H. B. Schlegel, G. E. Scuseria, M. A. Robb, J. R. Cheeseman, G. Scalmani, V. Barone, G. A. Petersson, H. Nakatsuji, X. Li, M. Caricato, A. Marenich, J. Bloino, B. G. Janesko, R. Gomperts, B. Mennucci, H. P. Hratchian, J. V. Ortiz, A. F. Izmaylov, J. L. Sonnenberg, D. Williams-Young, F. Ding, F. Lipparini, F. Egidi, J. Goings, B. Peng, A. Petrone, T. Henderson, D. Ranasinghe, V. G. Zakrzewski, J. Gao, N. Rega, G. Zheng, W. Liang, M. Hada, M. Ehara, K. Toyota, R. Fukuda, J. Hasegawa, M. Ishida, T. Nakajima, Y. Honda, O. Kitao, H. Nakai, T. Vreven, K. Throssell, J. A. Montgomery, Jr., J. E. Peralta, F. Ogliaro, M. Bearpark, J. J. Heyd, E. Brothers, K. N. Kudin, V. N. Staroverov, T. Keith, R. Kobayashi, J. Normand, K. Raghavachari, A. Rendell, J. C. Burant, S. S. Iyengar, J. Tomasi, M. Cossi, J. M. Millam, M. Klene, C. Adamo, R. Cammi, J. W. Ochterski, R. L. Martin, K. Morokuma, O. Farkas, J. B. Foresman, and D. J. Fox, Gaussian, Inc., Wallingford CT, 2016.

[38] Hohenberg, P., & Kohn, W. (1964). Inhomogeneous electron gas. *Physical review*, *136*(3B), B864.

[39] Kohn, W., & Sham, L. J. (1965). Self-consistent equations including exchange and correlation effects. *Physical review*, *140*(4A), A1133.

[40] Parr, R. G. (1980). Density functional theory of atoms and molecules. In *Horizons of quantum chemistry* (pp. 5-15). Springer, Dordrecht.

[41] Vydrov, O. A., & Scuseria, G. E. (2006). Assessment of a long-range corrected hybrid functional. *The Journal of chemical physics*, *125*(23), 234109.

[42] Vydrov, O. A., Heyd, J., Krukau, A. V., & Scuseria, G. E. (2006). Importance of short-range versus long-range Hartree-Fock exchange for the performance of hybrid density functionals. *The Journal of chemical physics*, *125*(7), 074106.

[43] Vydrov, O. A., Scuseria, G. E., & Perdew, J. P. (2007). Tests of functionals for systems with fractional electron number. *The Journal of chemical physics*, *126*(15), 154109.

[44] Grimme, S., Ehrlich, S., & Goerigk, L. (2011). Effect of the damping function in dispersion corrected density functional theory. *Journal of computational chemistry*, *32*(7), 1456-1465.

[45] Krishnan, R. B. J. S., Binkley, J. S., Seeger, R., & Pople, J. A. (1980). Self-consistent molecular orbital methods. XX. A basis set for correlated wave functions. *The Journal of chemical physics*, *72*(1), 650-654.

[46] Goerigk, L., Kruse, H., & Grimme, S. (2011). Benchmarking density functional methods against the S66 and S66x8 datasets for non-covalent interactions. *ChemPhysChem*, *12*(17), 3421-3433.

[47] DiLabio, G. A., Johnson, E. R., & Otero-de-la-Roza, A. (2013). Performance of conventional and dispersion-corrected density-functional theory methods for hydrogen bonding interaction energies. *Physical Chemistry Chemical Physics*, *15*(31), 12821-12828.

[48] Roithová, J., Ricketts, C. L., & Schröder, D. (2009). Reactions of the dications C7H62+, C7H72+, and C7H82+ with methane: Predominance of doubly charged intermediates. *International Journal of Mass Spectrometry*, *280*(1-3), 32-37.

[49] Roithová, J., & Schröder, D. (2007). Bond-formation versus electron transfer: C–C-Coupling reactions of hydrocarbon dications with benzene. *Physical Chemistry Chemical Physics*, *9*(6), 731-738.

[50] Roithová, J., & Schröder, D. (2007). Bimolecular reactions of molecular dications: reactivity paradigms and bond-forming processes. *Physical Chemistry Chemical Physics*, *9*(19), 2341-2349.

[51] Ricketts, C. L., Schröder, D., Roithová, J., Schwarz, H., Thissen, R., Dutuit, O., Žabka, J., Herman, Z.& Price, S. D. (2008). Competition of electron transfer, dissociation, and bond-forming processes in the reaction of the CO 2 2+ dication with neutral CO 2. *Physical Chemistry Chemical Physics*, *10*(33), 5135-5143.

[52] Roithová, J., Herman, Z., Schröder, D., & Schwarz, H. (2006). Competition of proton and electron transfers in gas-phase reactions of hydrogen-containing dications CHX2+ (X= F, Cl, Br, I) with atoms, nonpolar and polar molecules. *Chemistry–A European Journal*, *12*(9), 2465-2471.

[53] Ascenzi, D., Tosi, P., Roithová, J., Ricketts, C. L., Schröder, D., Lockyear, J. F.& Price, S. D. (2008). Generation of the organo-rare gas dications HCCRg2+ (Rg= Ar and Kr) in the reaction of acetylene dications with rare gases. *Physical Chemistry Chemical Physics*, *10*(47), 7121-7128.

[54] M. S. B. Munson, "Ionic reactions in gaseous amines", *J. Phys. Chem.*, **70**, 2034-2038(1966)

[55] E. G. Jones and A. G. Harrison, "Ion-molecule reactions in gaseous methyl amine", *Can. J. Chem*., 45, 3119-3128(1967)

[56] Wilson, P. F., Milligan, D. B., Lam, L. W., Freeman, C. G., Meot-Ner, M., & McEwan, M. J. (2002). Reactions of $CH_3OCH_2^+$ with hydrocarbons and O, N, and S compounds: applications for chemical ionization in selected ion flow tube studies. *Journal of the American Society for Mass Spectrometry*, *13*(9), 1028-1033

[57] W. Y. Feng and C. Lifshitz, "Influence of multiple hydrogen bonding on reactivity: ion/molecule reactions of proton-bound 12-crown-4 ether and its mixed cluster with ammonia and methanol", *J.Am. Chem. Soc.*, **117**, 11548-11554(1995)

[58] Anicich, V. G. (2003). An index of the literature for bimolecular gas phase cation-molecule reaction kinetics. http://hdl.handle.net/2014/7981

[59] Leach, S., Schwell, M., Jochims, H. W., & Baumgartel, H. (2006). VUV photophysics of acetic acid: Fragmentation, fluorescence and ionization in the 6–23 eV region. *Chemical physics*, *321*(1-2), 171-182.

[60] Holmes, J. L. (1973). The mass spectra of carboxylic acids—VI: Metastable dissociations of isomeric ions in the mass spectra of oxalic and formic acids, and malonic and acetic acids. *Organic Mass Spectrometry*, 7(3), 341-346.

[61] Borodin, A., Yamazaki, M., Kishimoto, N., & Ohno, K. (2005). Collision-Energy-Resolved Penning Ionization Electron Spectroscopy of HCOOH, CH_3COOH, and $HCOOCH_3$ by Collision with He*(23S) Metastable Atoms. *The Journal of Physical Chemistry A*, 109(21), 4721-4727.

[62] Schwell, M., Leach, S., Hottmann, K., Jochims, H. W., & Baumgärtel, H. (2001). He I photoelectron spectroscopy of formic acid isotopomers HCOOH and DCOOD. *Chemical Physics*, *272*(1), 77-90.

[63] Schwell, M., Dulieu, F., Jochims, H. W., Fillion, J. H., Lemaire, J. L., Baumgärtel, H., & Leach, S. (2002). Photophysical Studies of Formic Acid in the Vacuum UV: Fragmentation, Fluorescence, and Ionization in the 6− 23 eV Photon Energy Range. *The Journal of Physical Chemistry A*, *106*(45), 10908-10918.

[64] Siggel-King, M. R., Yencha, A. J., King, G. C., Malins, A. E., & Eypper, M. (2012). Formic and acetic acid: Valence threshold photoelectron and photoionization total ion yield studies. *Journal of Electron Spectroscopy and Related Phenomena*, 185(8-9), 204-210.

[65] Polášek, M., Zins, E. L., Alcaraz, C., Žabka, J., Křížová, V., Giacomozzi, L., Tosi, P., & Ascenzi, D. (2016). Selective Generation of the Radical Cation Isomers $[CH_3CN]^{\bullet+}$ and $[CH_2CNH]^{\bullet+}$ via VUV Photoionization of Different Neutral Precursors and Their Reactivity with C_2H_4. *The journal of physical chemistry. A*, *120*(27), 5041-5052.

[66] Ascenzi, D., Romanzin, C., Lopes, A., Tosi, P., Žabka, J., Polášek, M., Shaffer,C., & Alcaraz, C. (2019). State-selected reactivity of carbon dioxide cations (CO2+) with methane. *Frontiers in chemistry*, *7*, 537.

[67] Cernuto, A., Lopes, A., Romanzin, C., Cunha de Miranda, B., Ascenzi, D., Tosi, P., Tonachini, G., Maranzana, A., Polášek, M., Žabka, J. et al. (2017). Effects of collision energy and vibrational excitation of CH 3+ cations on its reactivity with hydrocarbons: But-2-yne CH_3CCCH_3 as reagent partner. *The Journal of chemical physics*, *147*(15), 154302.

[68] https://webbook.nist.gov/cgi/cbook.cgi?ID=C74895&Units=SI&Mask=20#Ion-Energetics

[69] Darla, N., & Sitha, S. (2019). Reaction between NH_3 ($\tilde{X}$1A1) and CO (X1Σ+): A Computational Insight into the Reaction Mechanism of Formamide (H_2N–CHO) Formation. *The Journal of Physical Chemistry A*, *123*(41), 8921-8931.

[70] Sun, F., Xie, M., Zhang, Y., Song, W., Sun, X., & Hu, Y. (2021). Spectroscopic evidence of the C–N covalent bond formed between two interstellar molecules (ISM): acrylonitrile and ammonia. *Physical Chemistry Chemical Physics*.

[71] Jeanvoine, Y., Largo, A., Hase, W. L., & Spezia, R. (2018). Gas phase synthesis of protonated glycine by chemical dynamics simulations. *The Journal of Physical Chemistry A*, *122*(3), 869-877.

[72] Scuderi, D., Pérez-Mellor, A., Lemaire, J., Indrajith, S., Bardaud, J. X., Largo, A., Jeanvoine Y. & Spezia, R. (2020). Infrared-Assisted Synthesis of Prebiotic Glycine. *ChemPhysChem*, *21*(6), 503-509.

[73] van der Rest, G., Jensen, L. B., Azeim, S. A., Mourgues, P., & Audier, H. E. (2004). Reactions of $[NH_3^{+\cdot}, H_2O]$ with carbonyl compounds: a McLafferty rearrangement within a complex?. *Journal of the American Society for Mass Spectrometry*, *15*(7), 966-971.

[74] van der Rest, G., Mourgues, P., Nedev, H., & Audier, H. E. (2002). A prototype for catalyzed amide bond cleavage: production of the $[NH_3, H_2O]^{\bullet+}$ dimer from ionized formamide and its carbene isomer. *Journal of the American Chemical Society*, *124*(19), 5561-5569.